11-9-2006

Uncovering the Role of Stress In Craniosynosostosis

Justin Heller
Yale University

Uncovering the Role of Stress
In
Craniosynosostosis

A Thesis Submitted to the
Yale University School of Medicine
in Partial Fulfillment of the Requirements for the
Degree of Doctor of Medicine

by

Justin B. Heller

Graduation Year of 2006

TABLE OF CONTENTS

ACKNOWLEDGEMENTS

The research projects described within are my own developed with guidance from Investigators: James Bradley, MD at UCLA and John Persing, MD at Yale University. I would also like to express my personal gratitude to Joubin Gabbay, MD a fellow researcher with whom a reciprocally collaborative and productive relationship was formed. We greatly assisted each other both in creative thought and the labor of our concurrent projects. The culmination of which though not described herein was achieving statistically significant healing (3D CT image shown below – Right image) of critically sized (white arrows) femoral defects with scaffolds developed by Joubin Gabbay and microdistractor stressed ADSC's described by myself. This has never before been accomplished with stem cells without the supplementation of exogenous growth factors (Scaffold plus unstressed stem cells -Left image). The coauthored paper is currently being submitted for publication and the clinical applications are being developed with the assistance of Macropore®.

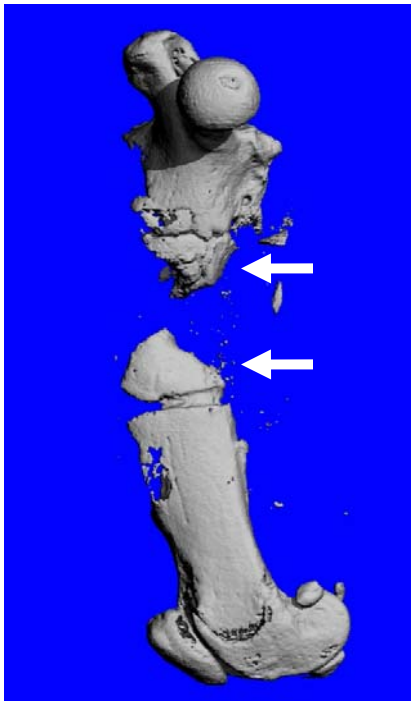

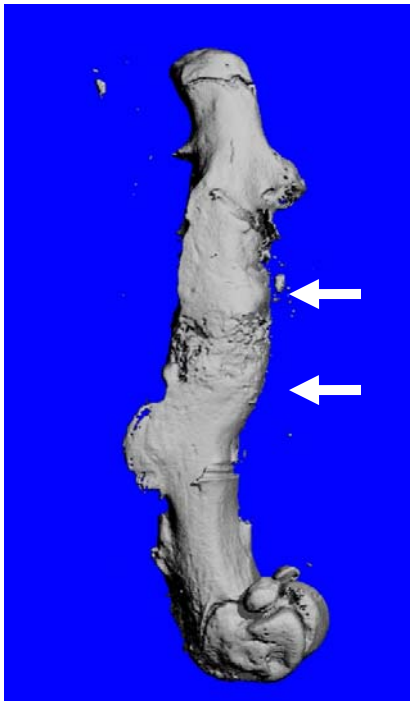

PREFACE

Craniosynostosis is the premature fusion of one or more of the cranial sutures resulting in skull deformity and possible brain dysfunction. It occurs in roughly 1 in 2,000 live births.[1] It may be associated with syndromes or occur sporadically. Any cranial suture may be involved.

The descriptions of the skull dysmorphologies have led to numerous hypotheses regarding the developmental trajectory of the synostosed skull, including the role of the cranial vault and cranial base. As proposed originally by Virchow (1851),[2] the shape of the skull in craniosynostosis is usually attributed to a lack of local growth perpendicular to the fused suture with compensatory growth occurring at adjacent patent sutures. This change in growth vectors is a variation on the highly coordinated adjustment required of the normally developing head. The reasons these growth vectors change may be directly related to changes in applied stress. However, the question still remains as to why the suture fuses prematurely.

The cause of premature fusion of cranial sutures has been speculated to be either due to physical constraint (i.e. stress)[3,4] or to genetic mutation.[5-8] Although some genetic mutations have been identified in individuals with craniosynostosis, the role of these mutations in pathways regulating suture patency and/or skull growth has not been characterized. To date, only coronal suture craniosynostosis has been found to be associated with a specific genetic mutation. Even still screens of non-syndromic patients with coronal craniosynostosis have found varied expression of this mutation, P250R – a fibroblast growth factor receptor (FGFR) 3.[9-12] In fact, only 50% of isolated cases of coronal synostosis have been shown to carry the mutation.[9-12] Current consensus is that

the FGFR3 mutation causes a particular syndrome (Muenke syndrome) with variable expressivity and incomplete penetrance.[11-12] As for the remaining majority of craniosynostosis cases no consensus exists.

The influence of physical constraint, or stress, is currently poorly understood. Despite studies suggesting that *in utero* constraint leads to craniosynostosis,[13,3,4] other studies concluded that constraint leads only to deformation of the skull while sutures remain patent.[14,15] Thus, we have a very limited understanding of the relationship between physical stress to suture fusion.

Genetic mutation and/or physical stress may play a role in causing premature suture fusion, but neither can affect the ontogenetic pathway of skull and sutures without having an impact on the entire craniofacial system. The osseous elements of the skull do not develop in isolation; rather the post-natal skull, brain, and dura mater develop in intimate physical and biochemical contact with one another. The precise nature of the interactions is unclear.

Many studies have demonstrated that the presence of dura mater is necessary to maintain suture patency, and further, that the signal mediating suture fusion involves soluble factors, rather than biomechanical factors or cell-cell interactions.[16-18] Additionally, studies have hypothesized that complex cell signaling from dura to osteogenic cell populations is responsible for patency of the suture.[16-20] However, the biomechanical/biochemical mechanisms necessary for production of cranial vault phenotypes in craniosynostosis are not elucidated by these findings.

A functional approach to the study of skull form was introduced by van der Klaauw (1948-1952)[21] and expanded on by Moss and colleagues.[22,23] In particular, Moss

and Young (1960)[22] presented a functional analysis to neurocranial growth, proposing that the size and shape of the cranial vault is determined by the form and orientation of the dura mater, which in turn is a direct reflection of the form of the brain. Citing Popa (1936),[24] Moss and Young (1960)[22] point out that the brain is encapsulated by the dura mater, which is firmly attached to the chondrocranium from its initiation. Since the dura mater and skull base are so firmly integrated at specific sites, a system of forces is produced by the growing brain, placing pressure against this capsule formed by the dura and skull tissues surrounding the brain. The dural folds produced by these attachments sites underlie the calvarial sutures and this relationship is proposed as playing a part in normal suture closure. Moss and Young (1960)[22] suggested biomechanical forces produced by growth of the brain as the means of communication between adjacent tissues.

The role of biomechanical forces in signaling diffusion of growth factors in communication among tissues has been supported experimentally,[25-31] suggesting both biochemical and biomechanical influences on the craniofacial phenotype. Whatever the mechanism for communication we know that a change in the growth trajectory of one of these tissue units influences changes in the trajectory of the others. For example, mechanical forces acting on the external neurocranium, such as binding of immature heads[32,33] or a habitual sleeping position,[34,35] changes the shape of the endocranium and neural mass. In fact, Babler and Persing et al. demonstrated that suture fusion shortly after birth via application of adhesive to the sagittal suture of rabbits causes both deformation of the basicranial and facial dimensions.[36] Likewise, changes in arrangement of dural attachment sites by way of cranial base deformation

(experimentally or naturally produced) alter the shape of the outer skull and the neural mass.[37,38] So, too changes in brain volume such as hydrocephalus, anencephaly, and microcephaly result in adjustments in neurocranial shape.[39-42]

In summary, one of the primary goals in the study of craniosynostosis is to determine the cause of premature suture fusion and its relationship to observed craniofacial dysmorphology. Beyond understanding the genetic mechanisms potentially underlying premature suture fusion, determination of the cause of craniosynostosis requires knowledge of the development of the entire craniofacial complex prior to, during, and following suture fusion. By the time children are diagnosed with craniosynostosis, the suture has already fused and the associated dysmorphology is well established. Thus, the data required to test directly hypotheses related to the cause of suture fusing is not available in humans and must be sought in animal models. Studies of human data are constrained to the more modest goal of acquiring a quantitative depiction of the phenotypes associated with suture fusion. Within this context, morphology and growth can be evaluated in individuals with craniosynostosis and the findings compared to perform clearer hypotheses to be tested in the appropriate animal models.

In this report, a new *in vitro* model (Microdistractor) is defined (Chapter 3) wherein a linear stress can be applied to a system. Our data suggests the Microdistractor device as effective for studying the cellular response to distraction stresses. As such a murine suture is stressed in this system and the histologic and gene expression changes are noted (Chapter 1). The application of oscillatory stress to cranial sutures results in fusion of both the posterior frontal and the normally patent sagittal suture. However, distractile stress did not cause fusion. This later finding is a likely result of the existence

of a range of acceptable stresses. Thus, the stress applied to the suture in distraction caused the two calvarial halves to undergo too great of separation for bony bridging to occur. Both stressed groups however, did demonstrate the same gene expression relative to control: significantly increased expression of the bone differentiation markers Runx2 and the late marker AP with nearly no expression of Noggin, a bone inhibitor. Thus, mechanical stress influenced the cells involved in sutural fusion and stimulated them to undergo osteogenic differentiation.

These findings were then compared with an animal (rabbit) model that spontaneously develops craniosynostosis *in utero* (Chapter 2). Our results suggest that pathologic rabbit coronal sutures progress toward complete suture fusion *in vitro*. Furthermore, the expression patterns of Noggin, Runx-2, and AP for a fusing suture paralleled that of our stressed model (Chaper 1). Thus, Noggin expression was decreased and Runx-2 and AP were increased in craniosynostosis.

Finally, pre-osteoblasts were biomechanically stressed within a collagen gel using the Microdistractor model (Chapter 4). Proliferative changes and genes of osteogenic differentiation were monitored. Cells undergoing linear distraction experienced rapid proliferation with a delayed expression of markers of osteogenic differentiation; whereas, cells undergoing oscillation had a rapid expression of osteogenic markers, but a cellular proliferation pattern indistinguishable from that of unstressed controls. These findings may help to explain the factors that occur in patients with craniosynostosis. For instance if a constant stress similar to distraction were to be applied a proliferative response would occur, when the stress is removed or oscillated the proliferated populations of cells may osteodifferentiate and lead to fusion.

At the end of this series we conclude that stress induces the same gene expression patterns as craniosynostosis and the particular pattern of stress application is crucial in determining the cellular response.

CHAPTER 1
IN-VITRO STRESS INDUCES CRANIOSYNOSTOTIC GENE EXPRESSION OF CALVARIAL SUTURES

Introduction: Current theory on normal cranial suture fusion entrusts the dura with the regulatory role. Studies suggest the dura responds to stress with changes in gene expression. Noggin (bone morphogenetic protein inhibitor) expression is decreased in normal (rat and murine) cranial suture fusion. However, its role in craniosynostosis and response to stress has not been studied. In our study, we investigated: 1) sutural fusion changes and 2) expression changes of Noggin and Runx2 in response to mechanical stress.

Methods: Posterior-frontal (fusing) and sagittal (patent) rat cranial sutures were held static, oscillated, or distracted for 10 days in an organ culture microdistraction device beginning at 5 days of age (10 days prior to onset of posterior frontal suture fusion)(n=15). Fusion scoring was given with 0 for patent, 1 fusing or partial fusion and 2 complete fusion. Percent fusion equaled the score received for bony closure. Expression of noggin, Run-X2, and AP was also localized by immunohistochemistry for all groups.

Results: Both the posterior frontal and sagittal suture demonstrated a statistically significant ($p<.05$) increase in fusion percentage with oscillation relative to the static control from 39% to 73% for the posterior frontal (fusing suture) and from 0% to 56% for the sagittal (patent suture) respectively. Immunohistochemistry of our static control demonstrated that Noggin was not expressed in the fusing posterior frontal suture, but expressed in the normally patent sagittal suture. Conversely, Runx2 was expressed in the PF suture, but not in the sagittal suture. However, when a mechanical stress was applied either via oscillation or distraction, both the posterior frontal and sagittal sutures expressed Runx2 but not Noggin as in the static fusing suture.

Conclusion: The application of oscillatory stress to cranial sutures results in fusion of both the posterior frontal and the normally patent sagittal suture. However, distractile stress did not cause fusion. This later finding is a likely result of the existence of a range of acceptable stresses. Thus, the stress applied to the suture in distraction caused the two calvarial halves to undergo too great of separation for bony bridging to occur. Both stressed groups however, did demonstrate the same gene expression relative to control: significantly increased expression of the bone differentiation markers Runx2 and the late marker AP with nearly no expression of Noggin. Thus, mechanical stress influenced the cells involved in sutural fusion and stimulated them to undergo osteogenic differentiation. Stress may therefore play a role in craniosynostosis.

INTRODUCTION

Craniosynostosis (the premature fusion of one or more cranial sutures) is one of the most frequently encountered craniofacial congenital disabilities occurring in 1 in 2000 live births.[43-45] Despite its prevalence, the etiology still remains largely unknown.

Normally, cranial sutures fuse through a process where the dura mater plays a key regulatory role. This concept was developed from experiments with the murine model wherein the posterior frontal suture reliably fused (Day 15 to Day 25), but the sagittal suture remained patent throughout life. Levine et al. demonstrated that suture translocation of the patent sagittal suture over the dura of the posterior frontal (PF) suture resulted in fusion.[46] Roth et al. confirmed this role by disrupting dura mater-suture continuity with placement of an impermeable Silastic membrane. He noted, the PF suture's fusion was significantly delayed and did not commence until Day 30.[47]

Localization and gene expression studies have demonstrated that three cytokines families, including fibroblast growth factor (FGF), transforming growth factor beta (TGF), and the bone morphogenic protein (BMP) are involved in cranial suture biology and their eventual fate.[48-53] Studies have shown these proteins to be inversely expressed by the dura of the fusing PF suture and patent sagittal suture.[48-58] In addition, Noggin (a BMP antagonist) is normally expressed in patent sutures but not in the normally fusing PF suture and Run-X2 (a marker of osteoblast differentiation) is normally expressed in fusing PF sutures.[59,60]

Gene expression of these regulatory proteins may also be influenced by mechanical stress. Ogle et al. applied a cyclical force to an in-vitro cranial suture model and noted that FGFR1 and FGFR2 expression increased.[61] Yu et al. noted that transient

stress applied to dura tissue resulted in a transient increase in FGF-2 and cellular permeability to Ca+2. He hypothesized that this increase resulted in gene expression changes.[62]

Cranial stresses experienced in fetal and early life may be associated with craniosynostosis.[63] In our study we looked at the response of cranial sutures to stress. A novel *in vitro* model was set up wherein rat cranial sutures (PF and sagittal) were harvested at post-natal (PN) day 5, (10 days prior to PF suture fusion), placed in a microdistractor and segregated to undergo oscillation, distraction, or be held static for 10 days. Outcomes were assessed at PN day 15 based on: 1) percentage of sutural fusion for both sutures and 2) immunohistochemistry expression changes of Noggin and Runx2.

METHODS

Dissection and Microdistractor Culture of Rat Calvaria

Sprague-Dawley pups were euthanized with an overdose of halothane at PN day 5. Animals were then submerged in a betadine bath and sterilized scissors were used to disassociate the head from the body. The head remained in the betadine bath for 40 seconds and then was rinsed in a final 70% alcohol bath for 10 seconds. Under a sterile hood, calvariae were removed aseptically with the sagittal, posterior frontal, and portion of the coronal sutures (Figure 1). Periosteum, and dura mater were left intact.

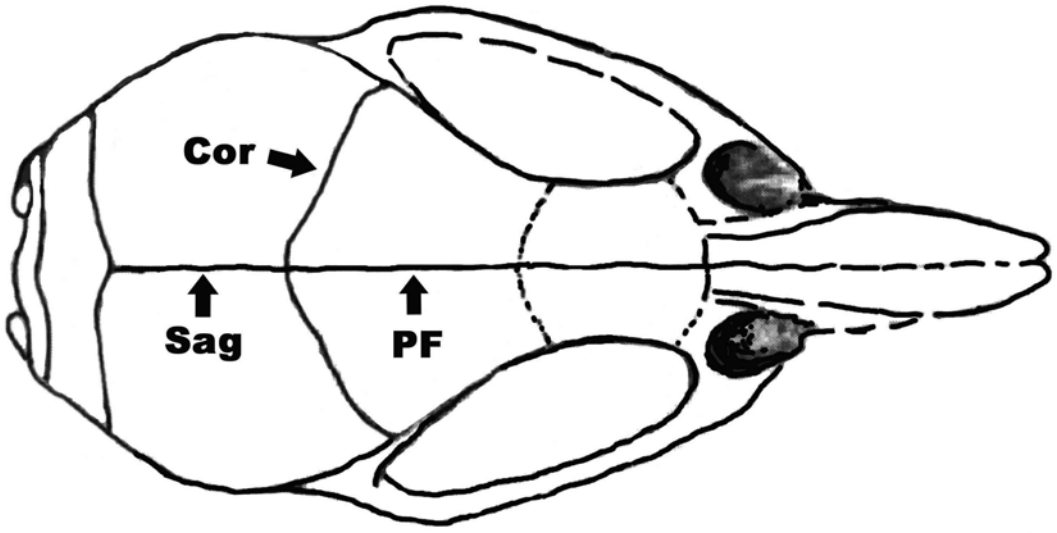

Figure 1. Line drawing of a Sprague dawley rat skull and cranial sutures. Sagittal suture (Sag), coronal suture (Cor) and posterior frontal suture (PF) are labeled with arrows designating the location of each cranial suture.

Next the calvaria, suture and dura block specimen was placed onto a microdistraction device. Prolene sutures were used to affix the calvarium at three points (frontal bone=1 and parietal bone=2) to a corrugated plastic scaffold (Figure 2). Cranial suture and corrugated plastic scaffold were then placed in a 150cc petri dish and positioned such that PF and sagittal sutures were perpendicular to the microdistractors axis of elongation/compression. Stainless steels pins (0.28 K-wires) were then passed through the microdistractor into the scaffolding to affix the microdistractor and sutures together as a unit.

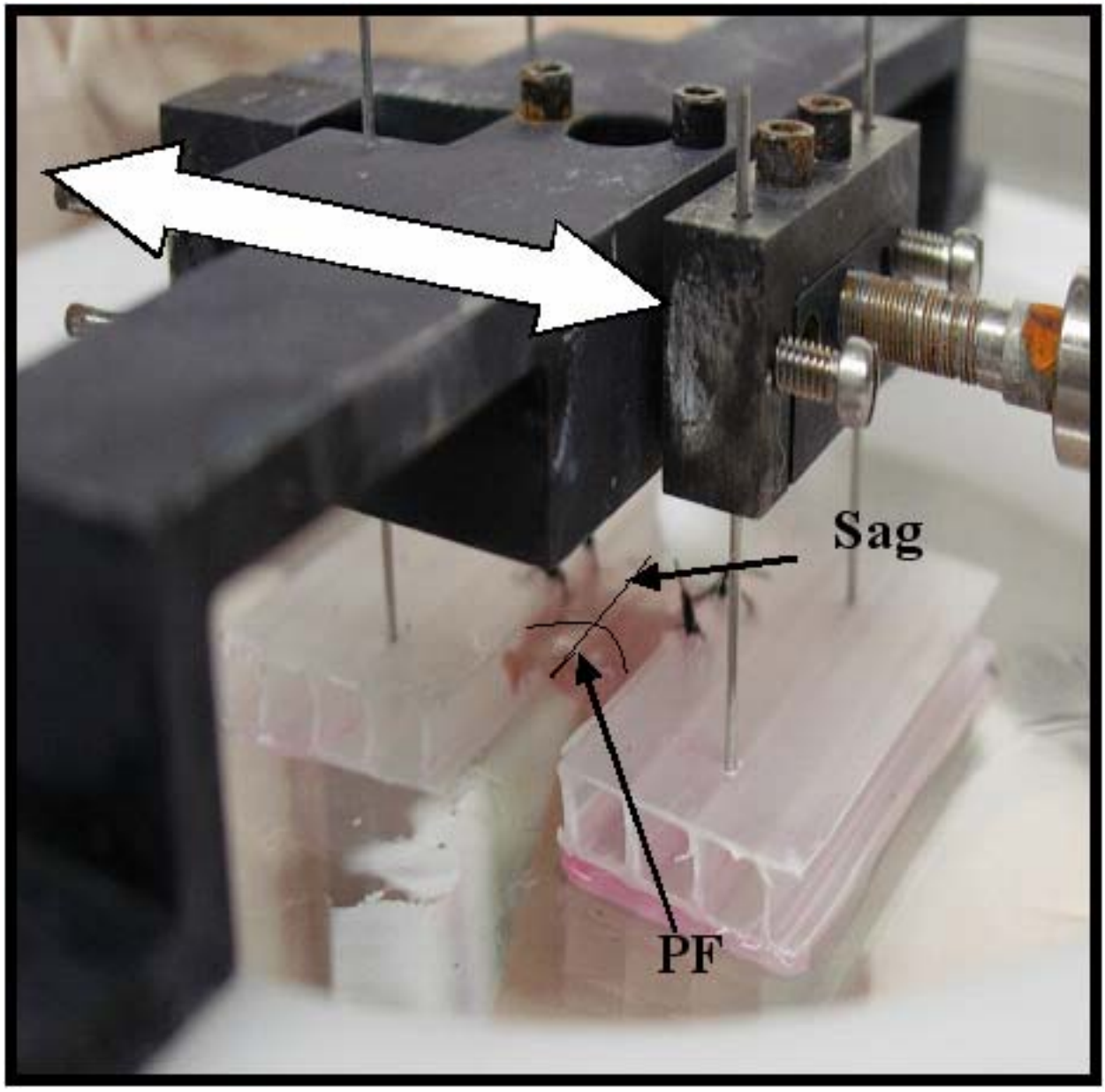

Figure 2. Cranial Sutures within Microdistractor: the PF and sagittal sutures are positioned to allow perpendicular stress with activation of the microdistractor.

Osteogenic media composed of 0.1 uM Dexamethasone, 50 uM ascorbic acid, 10 mM betaglycerol phosphate and 5% fetal bovine serum was then added to the dish such that the ectocranial surface of the suture was exposed to air but the endocranial was submersed in media. Media was changed daily for the duration of the experiment.

Experimental Groups

Experimental groups consisted of a static control group (Group 1), an oscillation group (Group 2) and a distraction group (Group 3).

For the static control group (Group 1), the microdistractor was not activated throughout the 10-day culture period. For the oscillation group (Group 2), gels were compressed one day and distracted the next day approximately 0.7mm about the neutral static position. For this oscillation process microdistractor activation was begun on day 1 and the cranial suture was compressed 0.7mm. For days 2 and 3 distraction of 0.7mm/ day was performed. For days 4 and 5, the suture was again compressed 0.7mm/ day. The cycle then continued to repeat alternating from compression to distraction until day 10. For the distraction group (Group 3), gel lengthening was performed at a rate of .18mm per day. Activation of the microdistractor device was begun on day 1 and carried through day 10.

Preparation of Tissues and Routine Staining

Specimens were fixed in 10% formalin, embedded in paraffin, and sectioned into 10 μm thick sections at 500 μm separation. Sections were carried anterior to posterior to 3000 μm for both the PF and sagittal sutures (7 sections). Five sutures from each group (static, oscillation, distraction) were processed in this manner (n=15). Sections were then stained with Harris' hematoxylin and eosin.

Immunohistochemical Localization of Noggin and RunX2

Briefly, seven 10 μm thick sections at 500 μm separation to 3000 μm for both the PF and sagittal sutures were processed for static, oscillation, and distraction groups (n=15). Sections were deparaffinized and taken through xylene and graded alcohols to

buffer. Antigens were unmasked through heating of sections in 10mM sodium citrate. Endogenous peroxidase activity was removed by preincubation of tissues in 1% hydrogen peroxide for 10 minutes. Blocking reagent was added for 1 hour at room temperature, slides were then incubated with the primary antibody, polyclonal rabbit antihuman Noggin and RunX-2 (ADI, San Antonio, TX) at 1:100 for 12 hours in a moist environment at 4°C, followed by biotinylated secondary antibody. For the controls, no primary antibody was added but the remainder of the steps was the same. The slides were then treated with avidin-biotin complex (Sigma, St. Louis, MO) and incubated with diaminobenzidine-tetrahydrochloride (Sigma). As such, areas of expression were seen as dark purple. Sections were lightly counterstained with methlene green for 15 seconds.

Fusion Percentage

Using an Axiovert 25 microscope (Zeiss ™Thornwood, NY) a Nikon Coolpix 4500 and a 23mm eye-piece adaptor (MVIA, Inc, Monaca, PA), images were taken (10X magnification). Fusion percentage was assessed by evaluating the serial 10μm H & E stained sections series from anterior to posterior for 3000μm (7 Sections) for both the posterior frontal and sagittal suture. Five specimens for each of the groups (static control, oscillation, and distraction) were evaluated by 3 blinded reviewers. For each section a "fusion score" was calculated by assigning a value of ‘0’, ‘1’, or ‘2’ to patent, fusing, and fused sections respectively. Suture fusion percent was calculated by dividing the actual fusion score by the maximum score possible times 100 (i.e., 7 sections each at 500μm intervals=maximum score of 14 if completely fused). This data was used to calculate overall fusion score. Statistical analysis was performed using a one-way analysis of variance for comparing percent suture fusion in each group. Inter-rater error was

calculated from comparison of overall score for each series of scores. Intra-rater error was also calculated based on comparison of fusion scores for 5 suture series given to the same reviewer three times spaced two weeks apart.

Noggin and RunX2 Expression Patterns

Digital immunohistochemistry images were taken of all sections at 10X magnification. Images included calvarium, osteogenic fronts, dura, and periosteum. KS-300 software (Zeiss™) was used for image analysis software was applied. Field was set to include osteogenic fronts, dura, and periosteum. Color of areas of expression was defined for each slide as was counterstain. A numerical density for expression was given. An expression ratio was then calculated for Runx2 and Noggin expression for oscillation and distraction relative to the corresponding suture of the static control. A student's t-test was used for statistical analysis of groups.

RESULTS

Fusion Percentage

With the posterior frontal suture (which normally undergoes the onset of fusion at PN day 15 and completes fusion by day 25) the static control showed a mean fusion percentage of 39.3% $\pm$ 4.7% at culture day 10 or PN day 15. Oscillation, showed significant increase in fusion percentage to 72.7% $\pm$ 6.1% ($p<.001$) at culture day 10 or PN day 15 (Figure 3). Thus, the fusion percentage was greater with oscillation (Group 2) compared to static control (Group 1). Distraction (Group 3) showed 0% fusion percentage ($p<.001$) at culture day 10 or PN day 15m (Fig 3). By culture day 10 the

distracted calvarial segments had been pulled apart almost 2 mm so it was not surprising that long fusion had not occurred.

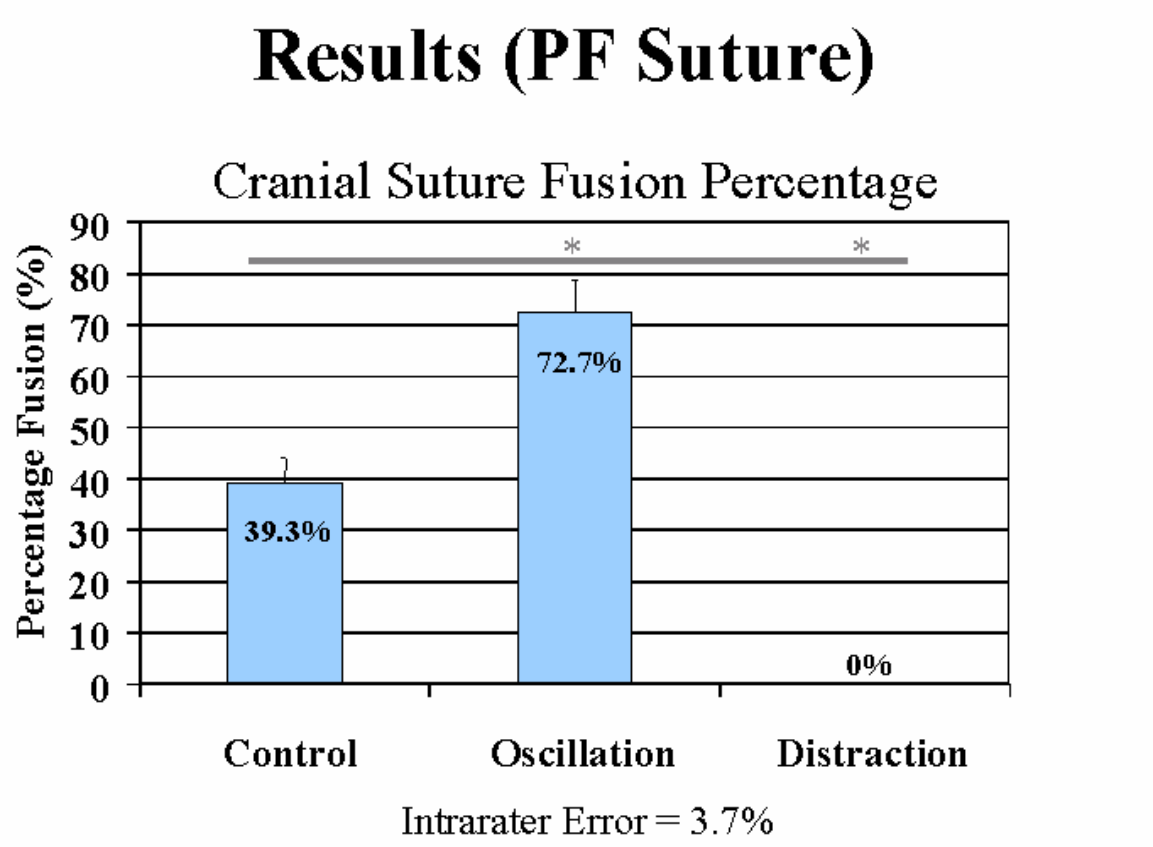

Figure 3. Posterior Frontal suture: percentage of suture fusion in control, oscillation and distraction groups. Oscillation showed a significant increase in fusion percentage compared to static control. Distraction showed 0% fusion percentage. * Denotes statistically significant compared to control.

With the sagittal suture (which normally maintains its patency throughout life) the static control demonstrated no fusion (0%) at culture day 10 or PN day 15. By contrast, oscillation had a mean fusion percentage of 56.0% $\pm$ 11.9% ($p < .001$) at culture day 10 or PN day 15 (Figure 4). Thus, over half of the patent sagittal sutures fused when subjected to oscillation in the microdistractors. Distraction (Group 3) showed no fusion (0%) at culture day 10 or PN day 15.

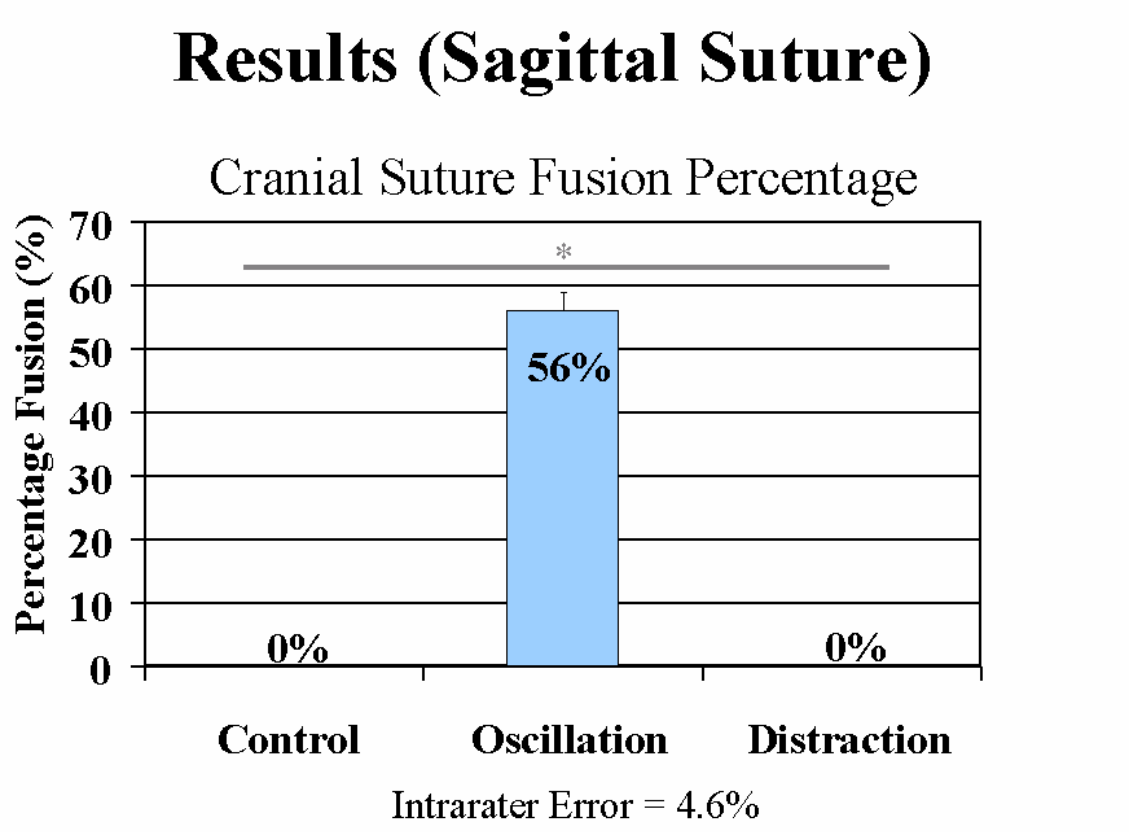

Figure 4. Sagittal suture: percentage of suture fusion in control, oscillation and distraction groups. Over half of the patent sagittal sutures fused when subjected to oscillation. * Denotes statistically significant compared to control.

RunX2 and Noggin Expression Patterns

For the PF (fusing) suture, the static controls (Group 1) did not express Noggin. The only visible Noggin expression was on the periosteum of ectocranial surface. By contrast, Runx2 was over-expressed in the same PF (fusing) static (control) sutures in the osteogenic fronts, dura, and periosteum.

For the (patent) sagittal suture, the static controls showed expression of Noggin throughout the osteogenic fronts, dura, and periosteum. By contrast, RunX2 was not expressed but only faintly identified in the periosteum of the ectocranial surface (Figure

5). Thus, an antagonistic expression pattern of Noggin and RunX2 was observed (ie. when Noggin was overly expressed then Run-x2 was underexpressed and vice versa).

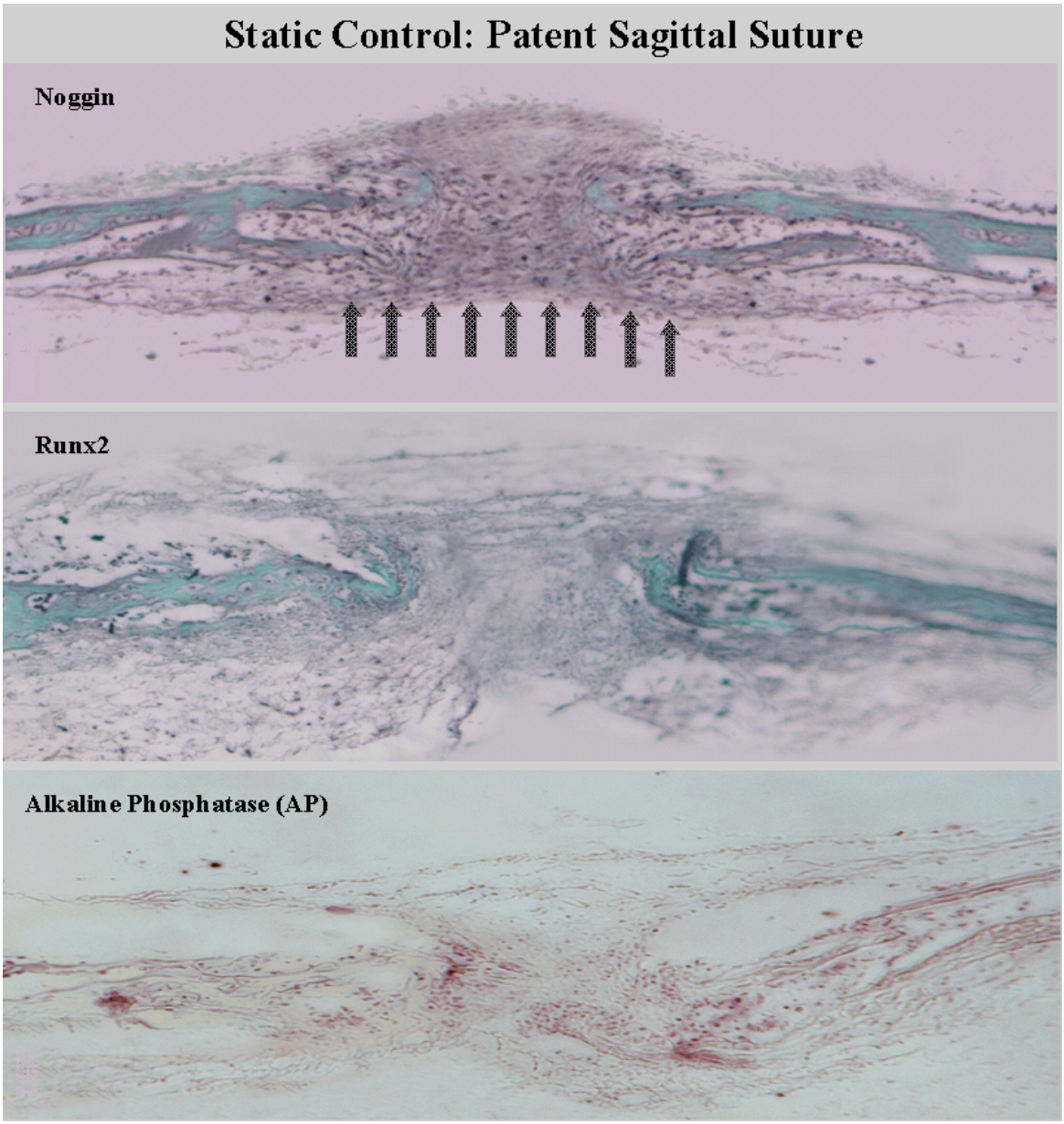

Figure 5. Static sagittal suture (Group 1). Noggin is expressed within sutural cells (↑) (upper panel) but Runx2 and alkaline phosphatase are not expressed (lower 2 panels).

With mechanical stress (Group 2 and Group 3) expressions patterns were the same for both oscillation and distraction. Noggin was not expressed or only minimally

expressed in both oscillation and distraction groups. Run-X2 had high expression in both stressed groups at the osteogenic fronts, dura, and periosteum (Figure 6). Thus, the PF (fusing) and sagittal suture which had opposite Noggin and Run-X2 expression in the static system had parallel Noggin and Run-X2 expression in the mechanical stress systems (Figure 7).

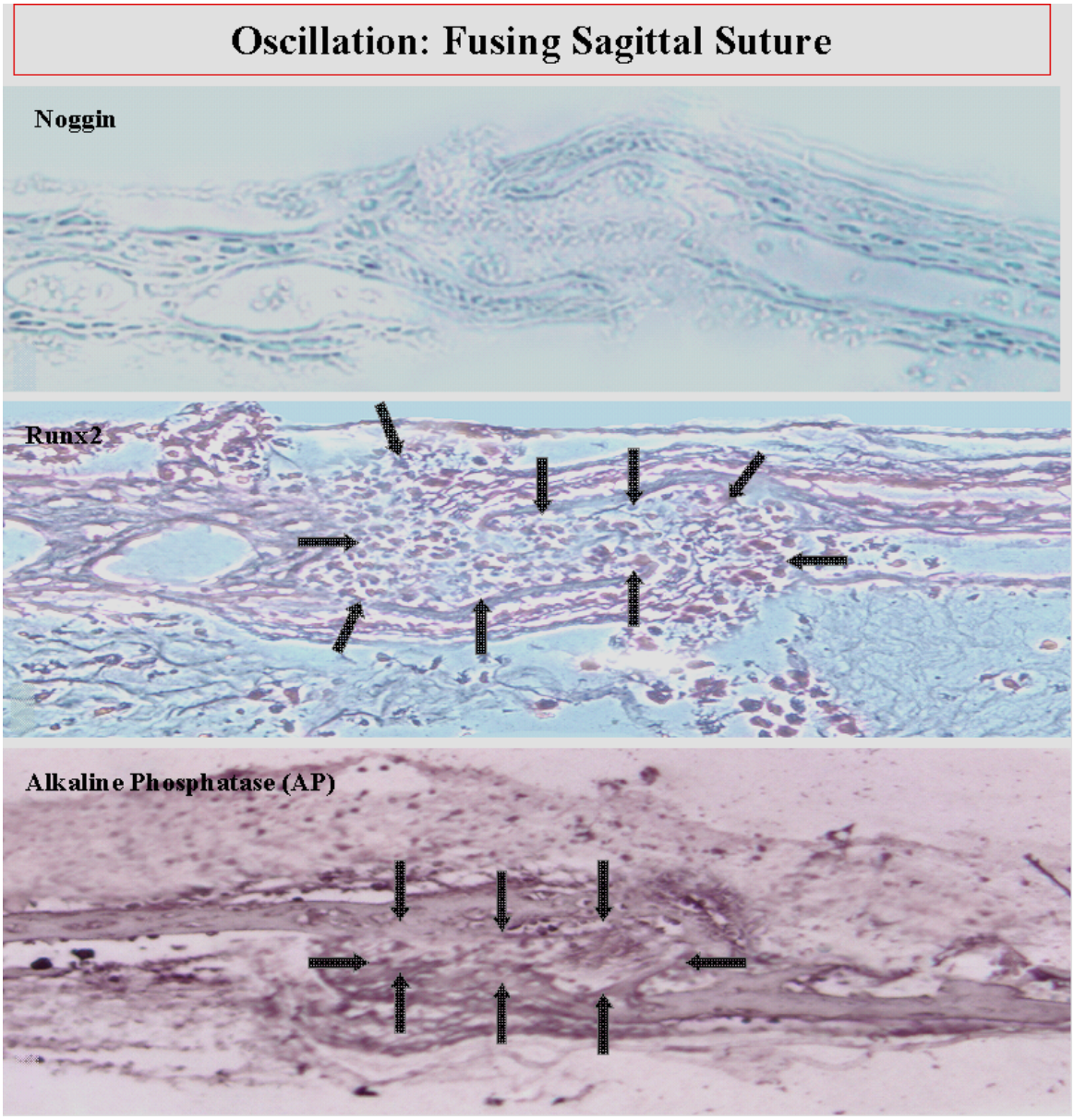

Figure 6. Oscillation stress (Group 2) of sagittal suture. Noggin is not expressed within cells (upper panel). Runx2 and alkaline phosphatase expression is seen in sutural cells (↑) (lower 2 panels).

Figure 7. Expression patterns of Noggin, Runx2 and AP in static control, oscillation and distraction groups for a) PF suture; and b) Sagittal suture. Red light represents under-expression and green light represents over-expression. Note antagonistic expression pattern of Noggin and RunX2. The PF and sagittal suture show opposing Noggin and RunX2 expression in the static system but parallel expression in the mechanical stress systems.

Quantative densitometry ratios confirmed these findings. For the static control the mean expression ratio of Noggin was 263 fold less for the PF relative to the sagittal suture. Also for the static control the mean expression ratio of Runx2 was 59 fold greater for the PF relative to the sagittal suture.

For the oscillation group the ratio of Noggin expression relative to the static control decreased by 70 fold for the PF suture and by 14,850 fold for the sagittal suture. Conversely, for the oscillation group the ratio of Runx2 compared to the static control showed an 8 fold increase in expression for the PF suture and a 63 fold increase for the sagittal.

For the distraction group the mean expression ratios were similar to the oscillation ratios relative to the static control. The expression of Noggin with distraction decreased 73 fold for the posterior frontal suture and by 15,028 for the sagittal suture. RunX2 expression increased 161 fold for the posterior frontal suture and 427 fold for the sagittal

suture. Thus, quantitative analysis of immunohistochemistry confirmed microscopic examination findings of decreased noggin and increased runX2 with mechanical stress.

DISCUSSION

Kirschner postulated that fetal stresses may be the inciting trigger that leads to the dura cytokine signaling involved with suture fusion and/or patency.[63] He showed that fetal constraint predictably led to craniosynostosis in mice. Biomechanical forces have also been postulated to influence the ultrastructure of human sagittal synostosis.[63-68] To test the response of cranial sutures to stress, an in vitro organ culture stress model was necessary. In our microdistraction model the calvarium, dura, and periosteum was subjected to regulated linear stresses. In this system oscillation stress caused an enhanced rate of fusion for the fusing PF sutures. In addition, oscillation stress even caused fusion in the normally patent sagittal suture. Thus, the fate of the sagittal suture was changed by the oscillating stress. With distraction stress augmentation of the osteogenic front was seen in both the PF suture and sagittal suture. However, neither of these sutures fused because of the imposed mechanical separation by the distraction. Within the osteogenic front increased expression of Run-X2 and decreased expression of Noggin was demonstrated.

Noggin is a BMP2/4 antagonist. Both BMP-2 and BMP-4 are present in the osteogenic fronts of fetal mice. BMP-2 declines after birth but BMP-4 expression continues.[66] BMP-4 is higher in suture mesenchyme than BMP-2 for both the sagittal and PF suture.[69] Stress increases BMP-4 expression.[68] Warren et al. described noggin's role in suture fusion noting that Noggin was expressed by the patent murine sagittal

suture but not by the fused posterior frontal suture. Furthermore, expression of Noggin was decreased by FGF2 and syndromic fgfr; and overexpression, induced by transfection, resulted in suture patency of the PF suture. These findings lead Warren et al. to postulate that Noggin expression plays a key regulatory role in cranial suture fusion and may play a role in craniosynostosis, or the premature fusion of cranial sutures.[59]

Runx2 is a transcription factor for the osteogenic differentiation proteins including osteocalcin and osteopontin. Activation occurs by BMP-4 binding to its receptor (BMPR-II), activating a smad signaling cascade, which in term dimerizes with runx2 resulting in transcriptional activation.[69] Park et al. localized Runx2 expression to the critical area of cranial suture fusion found in the osteogenic fronts and sutural mesenchyme.[60]

Our data showed that static controls demonstrated Noggin and Runx2 expression similar to those that occur in-vivo. When stress was applied, expression in both PF and sagittal suture paralleled that of a normally fusing suture (significant decrease in noggin expression and increase in runx2 expression). This suggested that a fusion-like environment was created by stress. Furthermore, stress induced a positive correlation between BMP-4 and Runx2 expression and a negative correlation between Runx2 and Noggin expression. Hence, the synergistic relationship between BMP-4 and Runx2 and anatagonist relationship between Noggin and Runx2 was confirmed by the application of stress. A precise measurement of applied stress is necessary to create a dose response curve for this microdistraction model.

In summary, the application of oscillatory stress to cranial sutures results in fusion of both the posterior frontal and the normally patent sagittal suture. However, distractile

stress did not cause fusion. This later finding is a likely result of the existence of a range of acceptable stresses. Thus, the stress applied to the suture in distraction caused the two calvarial halves to undergo too great of separation for bony bridging to occur. Both stressed groups however, did demonstrate the same gene expression relative to control: significantly increased expression of the bone differentiation markers Runx2 and Alkaline Phosphatase (AP) and reduced expression of the BMP antagonist Noggin. Thus, mechanical stress influenced the cells involved in sutural fusion and stimulated them to express genes of osteogenic differentiation. Stress may therefore play a role in craniosynostosis.

In the subsequent chapter (Chapter 2) the sutural gene expression of a rabbit model that develops craniosynostosis *in utero* is evaluated. By comparing these findings with the findings of this experiment we may better determine if stress causes gene expression similar to craniosynostosis.

CHAPTER 2
CRANIOSYNOSTOSIS GENE EXPRESSION CHANGES, AN ANIMAL MODEL

Introduction: Normal suture fusion has been shown to be driven by the molecular signals elucidated by the underlying dura. However, the pathogenesis of suture fusion in craniosynostosis is not well described. The purpose of our study was to examine the expression patterns of two important molecular signals (Noggin and Runx-2) in a cohort of congenital craniosynostotic rabbits, in order to gain a better understanding of suture behavior in craniosynostosis.

Methods: Coronal (fusing) and sagittal (patent) rabbit cranial sutures from a colony of congenitally synostosed rabbits and wild-type (control) rabbits were harvested at a neonatal time point. These sections were then grown in organ culture and harvested for histology at 0, 7 or 14 days of culture. Fusion percentage was then assessed and an overall fusion score was calculated. Expression of Noggin and Runx-2 was then localized by immunohistochemistry and quantified by western blot analysis.

Results: Histology of the wild-type cranial sutures (control) showed suture patency (score of 0%) for all coronal and sagittal sutures at 0 days, 7 days and 14 days of organ culture. Sagittal sutures of craniosynostotic animals also showed suture patency (score of 0%) at all culture times (0, 7 and 14 days). Of the 18 coronal sutures from the craniosynostotic animals, 8 remained patent and 10 fused. For the coronal sutures that fused, fusion scores of 14%, 41% and 84% were documented at 0, 7 and 14 days of organ culture, respectively. With immunolocalization, Noggin was found to be expressed in both the dura and suture cells underlying patent sutures, but not in fusing sutures *in vitro*. Runx-2 was found to be expressed in the dura beneath the suture and suture cells of fusing sutures, not patent sutures. Western blot densitometry confirmed these findings.

Conclusions: Our results suggest that pathologic rabbit coronal sutures progressed toward complete suture fusion *in vitro*; and expression patterns of Noggin and Runx-2 paralleled that of a well studied normal suture fusion model.

INTRODUCTION

Craniosynostosis, the premature fusion of calvarial sutures, occurs in approximately 1:2000 live births.[70] Research focused on the molecular mechanisms underlying normal cranial suture fusion has given clues to the pathologic condition. Normal suture fusion has been shown to be a complex process that is driven by the local dura, which supplies the molecular milieu directing the development of osteogenic precursor cells. The dura mater acts as a regionally specific endogenous tissue engineer elucidating growth factors such as IGF-1, FGF and TGF-Beta isoforms.

In addition to the effects of the locally released growth factors (FGFs, TGF-βs), cranial development has been shown to be influenced by the bone morphogenic proteins (BMPs).[71.72] Noggin, a secreted antagonist of BMP, has also been shown to be important in cranial suture development.[73] Runx-2, a transcription factor that is a marker of osteoblast differentiation, has been localized to the critical area of cranial suture fusion.[74] Runx-2 is found in the osteogenic fronts and sutural mesenchyme and has variable expressivity in patent vs. fusing sutures in normal development.

Both *in vivo* and *in vitro* studies on normal cranial suture fusion have shed light on underlying molecular cues, however, little is known about the condition in pathologic suture fusion or craniosynostosis. In order to better understand the pathology behind this process, it is essential to perform *in vivo* and *in vitro* studies on a craniosynostosis model. Currently the most representative animal model of this human condition is the rabbit craniosynostosis strain at the University of Pittsburgh. In this model, pathologic suture fusion begins *in utero* causing cranial vault deformities such as plagiocephaly in unilateral coronal suture synostosis and brachycephaly in bilateral synostosis.[75,76]

The purpose of our study was to examine the expression patterns of Noggin and Runx-2 in craniosynostotic rabbits. To do this, neonatal rabbit coronal and sagittal sutures were grown in organ culture and examined histologically for fusion, and the presence of Noggin and Runx-2 was analyzed with immunohistochemistry and western blot densitometry.

METHODS

Animals

New Zealand White Rabbits (Oryctolagus cuniculus) from an ongoing breeding colony of congenitally synostosed rabbits at the University of Pittsburgh, Department of Anthropology vivarium were used in our study. Morphologically, the rabbits from this colony with unilateral or bilateral coronal synostosis develop plagiocephaly or brachycephaly similar to human infants with these conditions (Figure 1). Wild-type (control) rabbits were also used.

Figure 1: Craniosynostotic rabbit from the ongoing breeding colony of congenitally synostosed rabbits at the University of Pittsburgh, Department of Anthropology vivarium. The arrow points to the Dome shaped brachiocephalic cranial vault, which forms secondarily to bilateral coronal craniosynostosis.

Cranial sutures were obtained from newborn rabbits (cranial suture formation began at approximately 17 days gestation; full term was 23-24 days gestation) (n=24). Two groups of newborn rabbits were studied: craniosynostotic (n=9) and wild-type controls (n=15). For the craniosynostotic rabbits a dominant maternal and dominant paternal craniosynostotic match was used in breeding.

Harvesting sutures

For our harvesting procedure the newborn rabbit pups were euthanized with an overdose of halothane. A sagittal scalp incision was used to expose the calvaria. A 10-blade scalpel was used to transect the cranial vault in an axial direction. The cranial sutures, dura and brain were included. Microscopic assisted dissection was used to divide each suture in half and create specimens measuring approximately 3mm x 3mm x 1.5mm. From each animal, 6 organ culture specimens (4 coronal sutures and 2 sagittal sutures) were created (n=144).

Organ Culture

Organ culture dishes (Falcon, Lincoln Park, N.J.), 60 x 15 mm, designed with a central well for media and surrounding moat for water, were placed into standard Petri dishes (Falcon) (Figure 2). BGJb (Gibco), a chemically defined, serum-free culture medium supplemented with penicillin G 100 ug/ml, streptomycin 0.1 mg/ml, amphotericin B 0.25 gm/ml, and ascorbate 1 gm/ ml (pH adjusted to 7.4 to 7.5 with 1.0 mol/liter NaOH) (all from Sigma, St. Louis, MO), was used to fill the central well. Wire mesh grid triangles (Wire Mesh Corporation, Los Angeles, CA) were sterilized and placed over the central well so that their undersurface was submerged in the medium. Calvariae with dura (excised as described above) were placed on the triangles and grown

at 37°C in 95% humidified air with 5% CO_2 for up to 30 days. The medium was changed every two days, at which time specimens were examined for signs of contamination. Specimens were harvested for histology at 0 days, 7 days, or 14 days of culture.

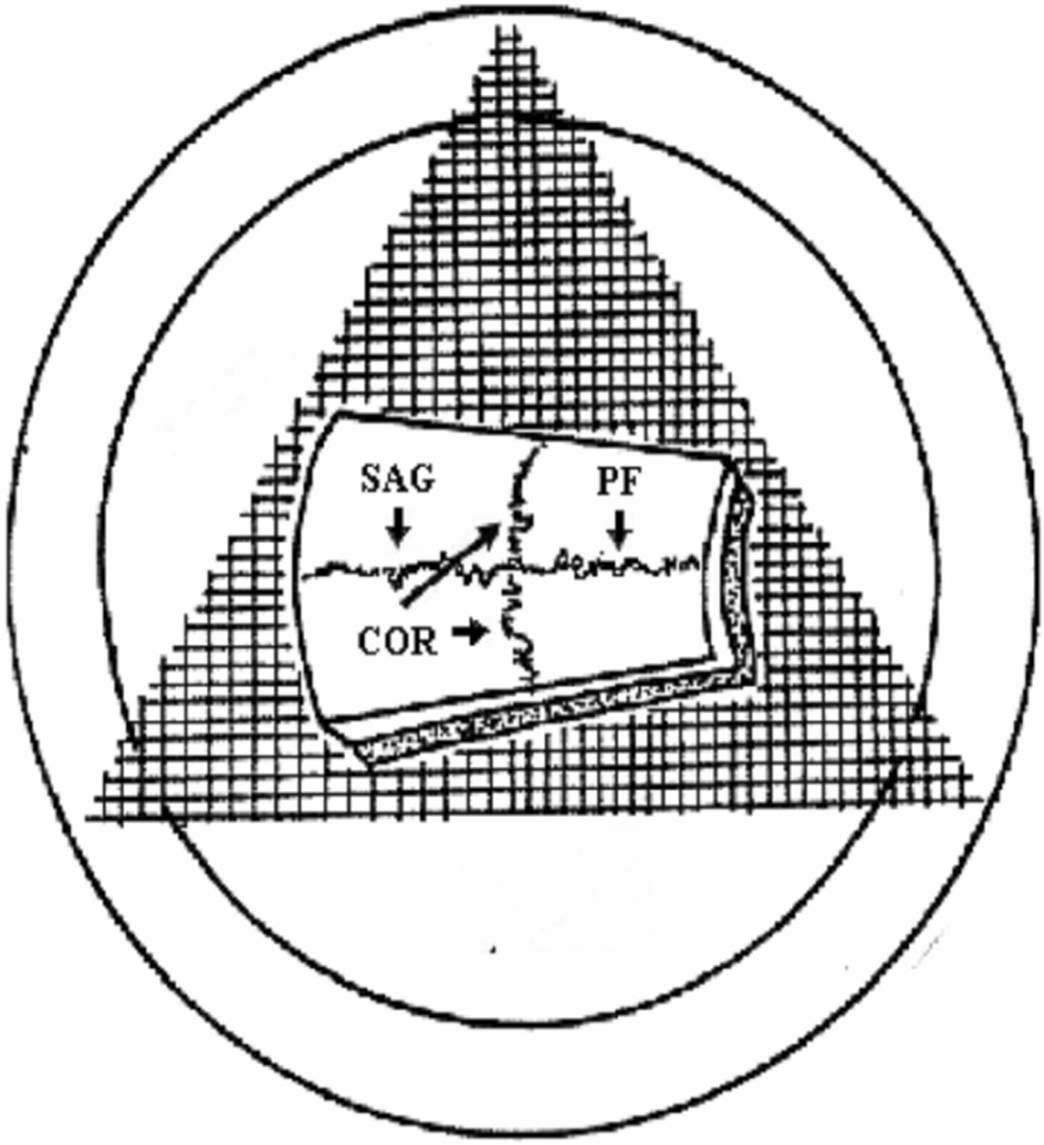

Figure 2: Representation of the organ culture system used in our study. In our study we divided the calvariae into separate isolated groups: one group examining the sagittal suture fusion and one group looking specifically at the coronal suture fusion.

Histology

Following harvest, the sutures were fixed in 10% formalin for 24 hours at 4°C, washed in distilled water, and decalcified in 5% EDTA-1 M phosphate-buffered saline solution (15mM phosphate, 150nM NaCl, 1% bovine albumin) for 72 hours. The specimens then underwent dehydration in graded ethanols and paraffin embedding. Four-micron-thick serial sections of each block were prepared. Routine hematoxylin and eosin staining was performed.

Fusion Percentage

Using an Axiovert 25 microscope (Zeiss™), a Nikon Coolpix 4500 and a 23mm eyepiece adaptor (MVIA, Inc, Monaca, PA), images were taken (10X magnification). Fusion percentage was assessed by evaluating the serial 10μm H & E stained sections series from medial to lateral for coronal sutures and anterior to posterior for sagittal sutures for 3000μm (7 Sections). Three blinded reviewers evaluated five sections from each specimen. For each section a "fusion score" was calculated by assigning a value of '0', '1', or '2' to patent, fusing, and fused sections respectively. Suture fusion percent was calculated by dividing the sum of fusion scores of each section by the maximum score possible times 100 (i.e., 7 sections each at 500μm intervals=maximum score of 14 if completely fused). This data was used to calculate overall fusion score. Statistical analysis was performed using a one-way analysis of variance to compare percent suture fusion for each suture. Inter-rater error was calculated from comparison of overall score for each series of scores. Intra-rater error was also calculated based on comparison of fusion scores for 5 suture series given to the same reviewer three times spaced two weeks apart.

Immunohistochemistry

Eight 10μm thick sections at 500μm separation to 3000μm for both the coronal and sagittal sutures were processed. Sections were deparaffinized and taken through xylene and graded alcohols to buffer. Antigens were unmasked through heating of sections in 10mM sodium citrate. Endogenous peroxidase activity was removed by preincubation of tissues in 1% hydrogen peroxide for 10 minutes. Blocking reagent was added for 1 hour at room temperature, slides were then incubated with the primary antibody, polyclonal rabbit antihuman Noggin and Runx-2 (ADI, San Antonio, TX) at 1:100 for 12 hours in a moist environment at 4°C, followed by biotinylated secondary antibody. For the controls no primary antibody was added, but the remainder of steps were the same. The slides were then treated with avidin-biotin complex (Sigma) and incubated with diaminobenzidine-tetrahydrochloride (Sigma). As such, areas of expression were seen as dark purple. Sections were lightly counterstained with methylene green for 15 seconds.

Western Blot Analysis

Briefly, equal amounts of proteins in each sample were resolved in 10% sodium dodecyl sulfate polyacrylamide gel electrophoresis (SDS-PAGE) and the proteins transferred onto PVDF membranes. After blocking with non-fat dried milk, the membranes were incubated with the appropriate dilution of primary antibodies. The membranes were then incubated with a horseradish peroxidase-conjugated secondary antibody. Statistical analysis was performed using a t-test to test for differences in the relative density of Noggin and Runx-2 between patent and fused sutures.

RESULTS

There were no infections in the organ cultures of both the 7-day and 14-day specimens. Routine histology of the wild-type cranial sutures (control) showed suture patency (score of 0%) of all coronal and sagittal sutures at 0 days, 7 days and 14 days of organ culture. Sagittal sutures of craniosynostotic animals also showed suture patency (score of 0%) at all culture times (0, 7 and 14 days).

For the craniosynostotic animals, both coronal sutures from 2 animals developed suture fusion *in vitro* (brachycephaly *in vivo*). Only one of the coronal sutures from 6 animals developed suture fusion *in vitro* (plagiocephaly from unilateral coronal synostosis *in vivo*). Neither coronal suture from one animal developed suture fusion (normocephalic *in vivo*). Thus, of the 18 coronal sutures from the craniosynostotic animals 8 remained patent and 10 fused. For the coronal sutures that fused, an initial fusion score of 14% was noted at 0 days of culture. A fusion score of 41% was documented at 7 days of culture and a fusion score of 84% was documented at 14 days of culture (Figure 3). Thus, pathologic suture fusion progressed in an *in vitro* system.

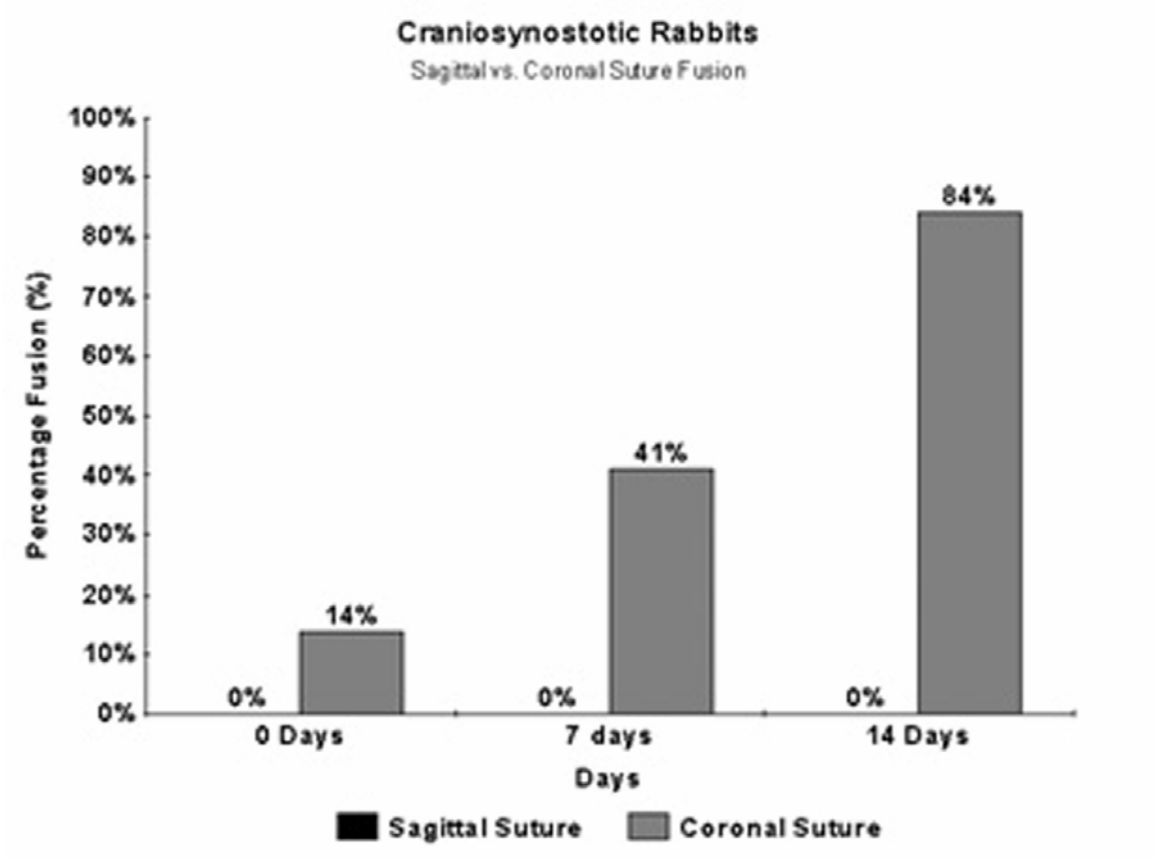

Figure 3: Percent fusion observed in the sagittal sutures and fusing coronal sutures in the craniosynostotic rabbit model at three time intervals: 0 days, 7 days and 14 days. The sagittal suture remained patent at all cultures times. For the coronal sutures that fused, suture fusion progressed in the *in vitro* system.

Expression patterns of Noggin and Runx-2 were similar between *in vitro* patent sutures: sagittal, 'wild-type' coronal and non-fusing coronal sutures in craniosynostotic animals. However, with *in vitro* fusing coronal sutures from craniosynostotic animals, immunolocalization patterns were distinct. Noggin was expressed in patent *in vitro* sutures (Figure 4a). This marked expression was seen within cells of both the dura and fibrous suture regions. In contrast, Noggin was not expressed or showed minimal expression in fusing *in vitro* sutures of craniosynostotic animals (Figure 4b). This was true within cells of both dura and suture regions. Runx-2 expression was not observed

within dura beneath the suture or suture cells of patent sutures (Figure 5a). Within these specimens these markers were only seen in periosteal cells or dural cells adjacent to bone. In contrast, Runx-2 expression was seen in fusing *in vitro* sutures (Figure 5b). This expression on both markers was seen within dura and suture cells.

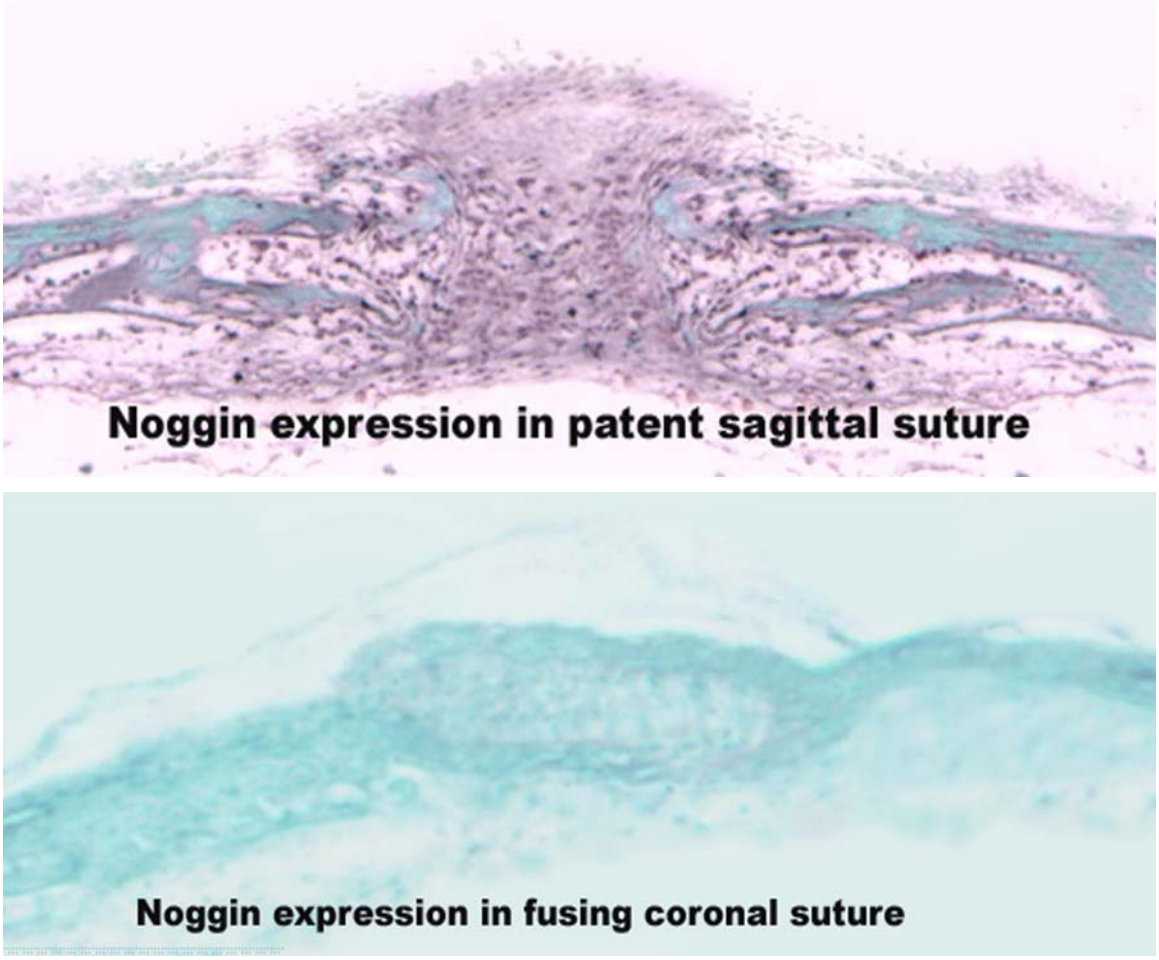

Figure 4: Expression pattern of Noggin in a) patent sagittal suture, and b) fusing coronal suture. Noggin was expressed in both the dura and suture cells underlying patent sutures but not in fusing sutures.

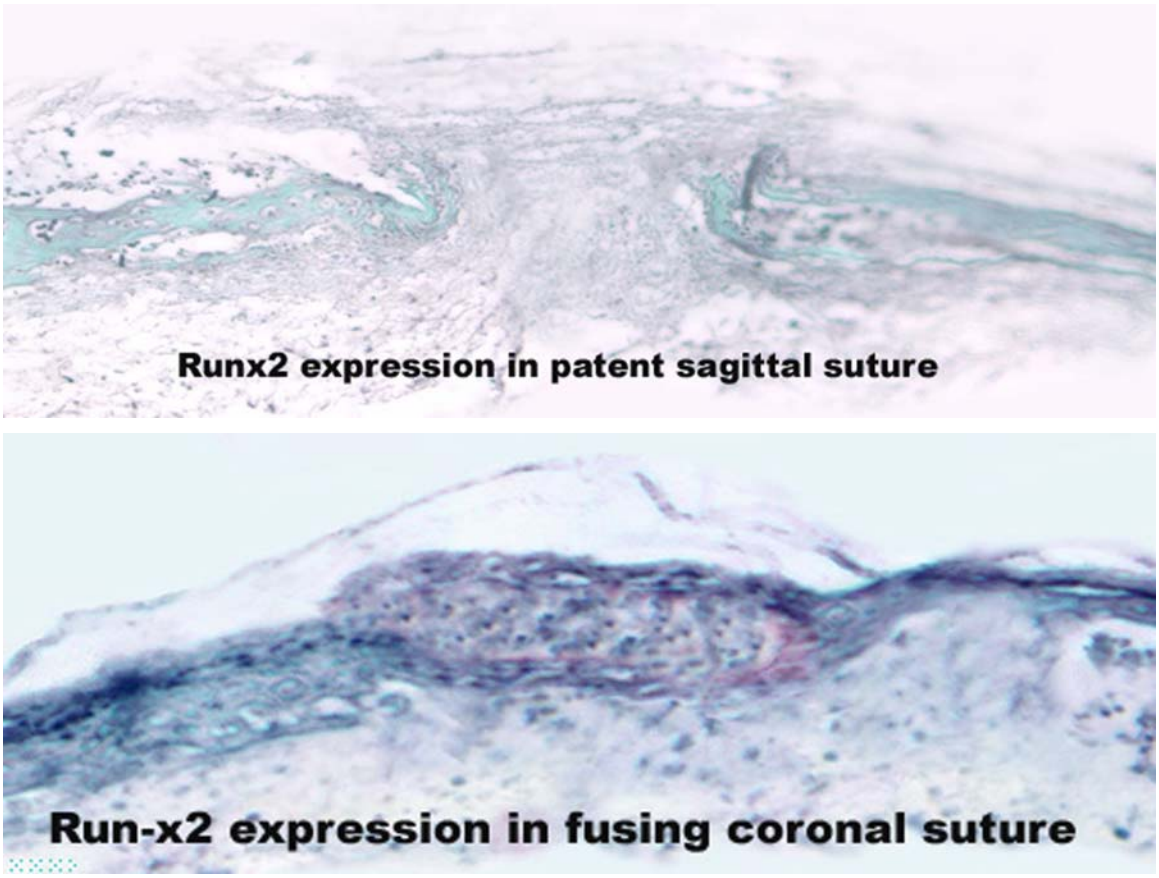

Figure 5: Expression pattern of Runx-2 in a) patent sagittal suture, and b) fusing coronal suture. Runx-2 was expressed in the dura beneath the suture and suture cells of fusing sutures but not patent sutures.

Western blot analysis showed a difference in Noggin and Runx-2 protein expression when patent and fusing sutures were compared (Figure 6). Fusing sutures had a significantly lower expression of Noggin protein when compared to patent sutures, with a relative density of 0.14 ($p<0.05$). Fusing sutures had a significantly higher expression of Runx-2 protein when compared to patent sutures, with a relative density of 3.16 ($p<0.05$).

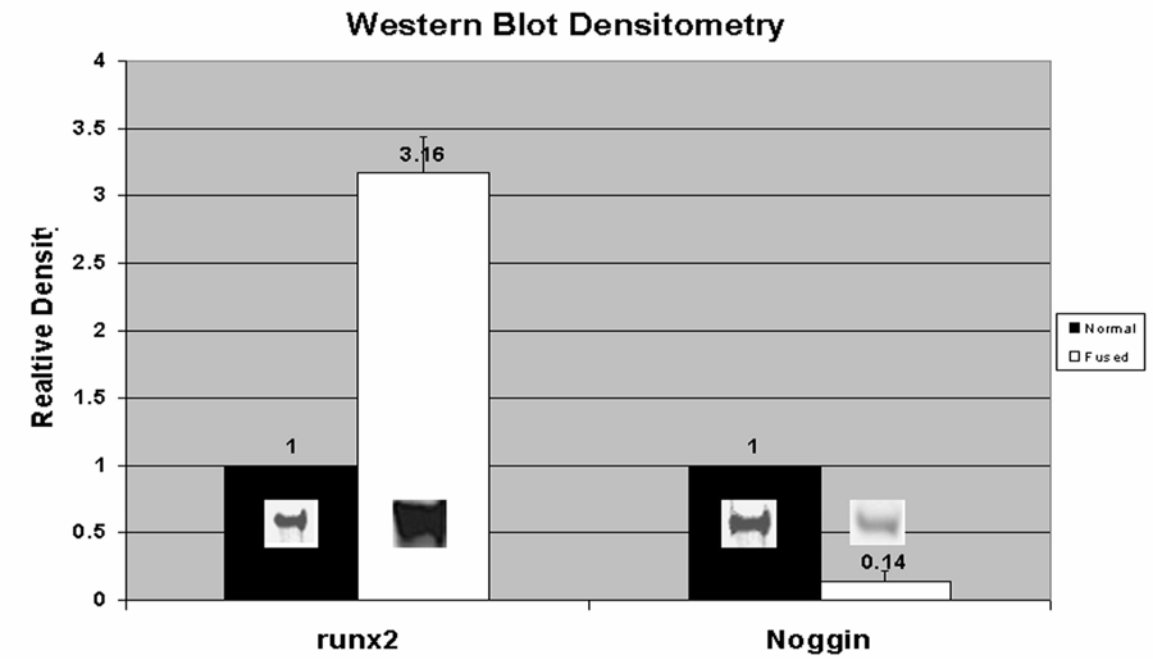

Figure 6: Relative densities of Noggin and Runx-2 in patent and fusing sutures as determined by western blot densitometry. Fusing sutures showed significantly lower Noggin expression and significantly higher Runx-2 expression when compared with patent sutures.

DISCUSSION

Previous studies have described *in vitro* models for normal cranial suture fusion. Bradley et al. showed that in an organ culture system, murine posterior frontal cranial suture fusion occurred in a similar fashion to the live mouse but in a delayed fashion (*in vitro* posterior frontal suture fusion occurred between 29 and 46 days compared to 25 and 41 days for *in vivo* fusion). With the pathologic craniosynostotic rabbits, suture fusion begins prenatally shortly after suture formation. Using a similar organ culture model to the above murine *in vitro* model, we documented pathologic *in vitro* cranial suture fusion in the coronal suture of the rabbit. Our data showed that progression of suture fusion occurred in an *in vitro* system with neonatal coronal sutures of craniosynostotic animals.

In our study, dominant craniosynostotic rabbit parents had pups with plagiocephaly, unilateral coronal synostosis,[75] brachycephaly, bilateral coronal synostosis,[71] and normocephalic, patent sutures.[70] This was consistent with previous studies on this model.[75,76]

Studies have demonstrated that normal suture formation is directed by the paracrine action of the regional dura mater. Osteoinductive growth factors and cellular elements from the dura influence the overlying suture mesenchyme and the formation of osteogenic fronts.[77-79] Evidence suggests that there are at least three growth factor families that are closely involved in cranial suture biology: bone morphogenetic proteins (BMPs), transforming growth factor-betas (TGF-βs), and fibroblast growth factors (FGFs).

The BMPs are secreted growth factors that are part of the TGF-β superfamily. The actions of these growth factors are highly concentration dependent and influence a number of cellular processes. For instance, BMPs have been shown to promote cellular chemotaxis and proliferation at low extracellular concentrations and to induce cellular differentiation and bone formation at high extracellular concentrations.[80,81]

Noggin is a BMP-2/4 antagonist. Both BMP-2 and BMP-4 are present in the osteogenic fronts of fetal mice. Warren et al. have examined postnatal suture mesenchyme in an attempt to determine Noggin's role in normal suture fusion in a murine model.[72] They found that Noggin was expressed by the patent sagittal suture but not by the fused posterior frontal suture. They also found that expression of Noggin was decreased by FGF2 and syndromic Fgfr; and that overexpression of Noggin, induced by transfection, resulted in suture patency of the normally fused PF suture. Our data

suggests an important role for Noggin in pathologic suture fusion as well. Underexpression of Noggin was found in the dura and coronal mesenchyme prior to suture fusion. In the same system control, patent coronal and sagittal sutures expressed Noggin.

Runx-2 (also known as Cbfa-1) is a master transcription factor that controls osteoblast differentiation and the maintenance of differentiated osteoblasts. Runx-2 is activated through a cascade, starting with BMP-4 binding to its receptor (BMPR-II) (Figure 7). This binding activates a SMAD signaling cascade, ultimately activating Runx-2 and stimulating osteogenic gene transcription.[82] Reflecting its major role in bone formation, Runx-2 levels have been shown to be elevated in areas of normal suture formation.[83] Our data showed that Runx-2 expression occurred during fusion of the coronal suture in craniosynostotic rabbits.

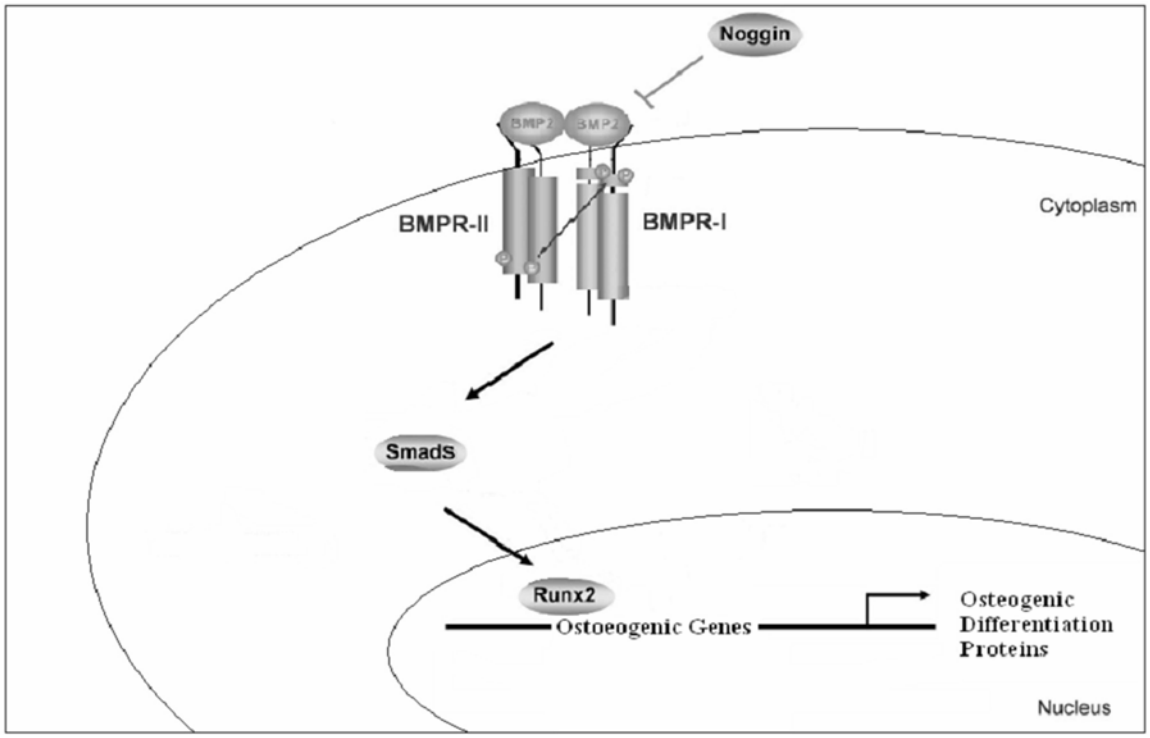

Figure 7: The role of Noggin and Runx-2 in BMP signaling.

Using the craniosynostosis model from the University of Pittsburgh and looking at osteogenic markers of dura and suture cells *in vitro*, our results concur with those that have been found in studies looking at normal suture development. Immunohistochemical evaluation demonstrated increased expression of Noggin in the patent sutures and marked underexpression of Noggin in the fused craniosynostotic sutures. Western blot densitometry confirmed these findings. Looking at Runx-2 expression in the craniosynostotic rabbit model we found overexpression of Runx-2 in the fused synostotic sutures when compared with the level found in the patent (normal) sutures.

In summary, pathologic rabbit coronal sutures progressed toward complete suture fusion *in vitro* and expression patterns of Noggin and Runx-2 paralleled that of a well-studied normal suture fusion model.

When we compare these findings to our previous *in vitro* stress model (Chapter 1) we note that the application of stress to a normally patent suture induced the same pattern of gene expression as noted in this craniosynostosis rabbit mode; this expression being a decrease in Noggin and an increase in Runx-2. In the subsequent chapter (Chapter 3) we further utilize our *in vitro* stress model but manipulate it such that cells may be seeded within a collagen gel and linearly stressed. The goal is to evaluate the role of stress on cells similar of early development (pre-osteoblasts). The proof of this linear application of stress by this model follows (Chapter 3) and later a description of the gene expression this stress has on pre-osteoblasts (Chapter 4).

CHAPTER 3
DEVELOPMENT OF AN IN-VITRO MODEL FOR UNIFORM APPLICATION OF STRESS

Introduction: Distraction osteogenesis has been used to correct hypoplastic and asymmetric bony deformities in the growing patient; yet its underlying cellular mechanisms are poorly understood. Using a new *in vitro* model, the microdistractor, morphologic properties of preosteoblasts under mechanical strain were studied.

Methods: Mouse calvarial MC3T3 cells were suspended in a polymerized three-dimensional collagen gel and stressed for 14 days as one of three groups (n=30): 1) Distraction (0.5mm/day); 2) Oscillation (1mm/day for 2 days alternated with 1mm/day for 2 days) and 3) Control (no force). A computer modeling system, KS-300, was used to record cell shape (aspect ratio) and orientation (deviance from axis of stress).

Results: In ***Part I*** of the study, morphologic cellular changes were found to be even throughout different regions of the gel (central versus peripheral, versus different vertical layers), suggesting the force was evenly applied to all cells in the gel. In addition, when linear distraction forces were applied, morphologic change occurred over time suggesting a morphological response to the applied stress. In ***Part II*** of the study, with different forces applied, morphologic changes occurred over time such that linear distraction forces caused cells to elongate and align in a parallel direction to the force whereas oscillation caused cells to switch from parallel (with distraction) to perpendicular (with compression) orientation relative to the force applied.

Conclusion: Our data suggest the microdistractor device is an effective *in vitro* model for studying the cellular response to distraction stresses. It may be used in future studies to optimize clinical methods of distraction.

INTRODUCTION

Distraction osteogenesis (DOG) of membranous bone has become an accepted modality in the correction of facial anomalies without bone grafts in growing patients.[84] Although much is known about bony healing and repair, the cellular mechanism of distraction osteogenesis is not fully understood. Mechanical stress has been shown to regulate bone production during distraction.[85] Stress across the distraction site may be an important part of the initiation of osteogenesis (cellular recruitment and organization), the remodeling of the bone regenerate, and the completion of bone consolidation. Such stress has also been hypothesized to play a potential role in the development of craniosynostosis, or the premature fusion of one or more sutures of the skull (see Preface).

Part of the difficulty in studying the effect of stress has been the paucity of effective *in vitro* models. Vacuum applied stress to monolayered cells has also been used to study the effect of biomechanical forces on osteoblasts (Flexercell Unit^{TM}).[86-93] However, this *in vitro* model does not distribute stress equally to the cells and has limitations inherent in a two-dimensional system (i.e. cell contact occurs in one plane only).[94] To better simulate the environment of *in vivo* distraction osteogenesis and craniosynostosis (i.e. linear stress), we created a model adapted from an *in vitro* system used to study the effect of tension forces on myofibroblasts.[95] In our model, cultured pre-osteoblasts may be distracted and stressed in a 3-D collagen gel.

In the present study, we aimed to: 1) characterize the morphologic changes of pre-osteoblasts that are subjected to linear stress, and 2) determine if morphologic changes were uniform throughout the 3-dimensional system. To do so, we embedded pre-

osteoblasts cultured from an immortalized cell line (MC3T3-E1) in a collagen gel. Mouse calvaria-derived MC3T3-E1 cells are used for studying differentiation along the osteoblast lineage.[96] Using these cells we compared morphologic changes of cells subjected to distraction, oscillation (distraction and compression) and no force (control). In addition, we compared morphology of cells within the same gel but in different layers or locations of the gel.

METHODS

Cell isolation and culture

The osteoprogenitor mice calvarial cells (MC3T3-E1: clone 4: ATCC, Manasses VA) were raised in Dulbecco's modified eagle's medium (DMEM: Sigma, St. Louis, MO), 10% fetal bovine serum (FBS, Summit Biotechnology, Ft. Collins, CO), penicillin (100U/ml: Invitrogen, Grand, Island, NY), and streptomycin (100ug/ml: Invitrogen). The cells were harvested between passages 18 through 28.

Preparation of collagen gels

A Delrin mold (McMaster Carr Supply Company,) was created to allow the liquid collagen to polymerize into a three dimensional shape (approximately 3cm x 3cm x 1.3cm). The sterile mold was housed in a large petri dish (100 mm X 15 mm) and sealed with silicon Stopcock grease (Dow Corning, Midland, MI). The petri dish was blocked with bovine serum albumin (BSA, 2g/ml, EM Science: Gibbstown, NJ) for 1 hr at 37^0C and rinsed with phosphate buffer saline (PBS) before use. Prior to pouring the collagen solution, two polyethylene bars (25mm X 5mm X 3mm) (Fisher Scientific, Fairlawn, NJ) were placed

at either end of the mold after being pretreated with sulfuric acid (96 hours) and distilled water (48 hours).

Collagen gels were prepared using monomeric Vitrogen 100 bovine skin collagen (3.0 mg/ml, Collagen Biomaterials, Palo Alto, CA). For each gel, 8.50 ml of Vitrogen 100 was mixed with 750□l of 10X Minimum Essential Medium (MEM: Life Technologies, Rockville, MD), 750□l of HEPES at ph 9.0 (Sigma), and 250-500ul of DMEM containing approximately 2 million suspended cells while in a 4^{o}C cold room. Five milliliters of the suspension was poured into the mold and was allowed to polymerize for 1 hour at 37^{0}C. The resulting gels contained about 1,000,000 cells (200,000 cells/ml) and were adherent to the porous polyethylene bars. Subsequently, the gel was sustained in DMEM, supplemented with 10% FBS, and 100□g/ml Penicillin and 100□g/ml Streptomycin.

Cellular viability within gels was assessed by light microscopic morphology. Live cells within a collagen gel have an elongated, fibroblast-like structure, whereas dead cells take on a rounded, shrunken structure. Percentage of cell death was calculated by assessment of total number of shrunken, rounded cells divided by the total number of cells within a microscopic field.

Microdistractor Design

After polymerization, the Delrin mold was removed and the microdistractor device was placed within the large petri dish parallel over the collagen gel (Figure 1).

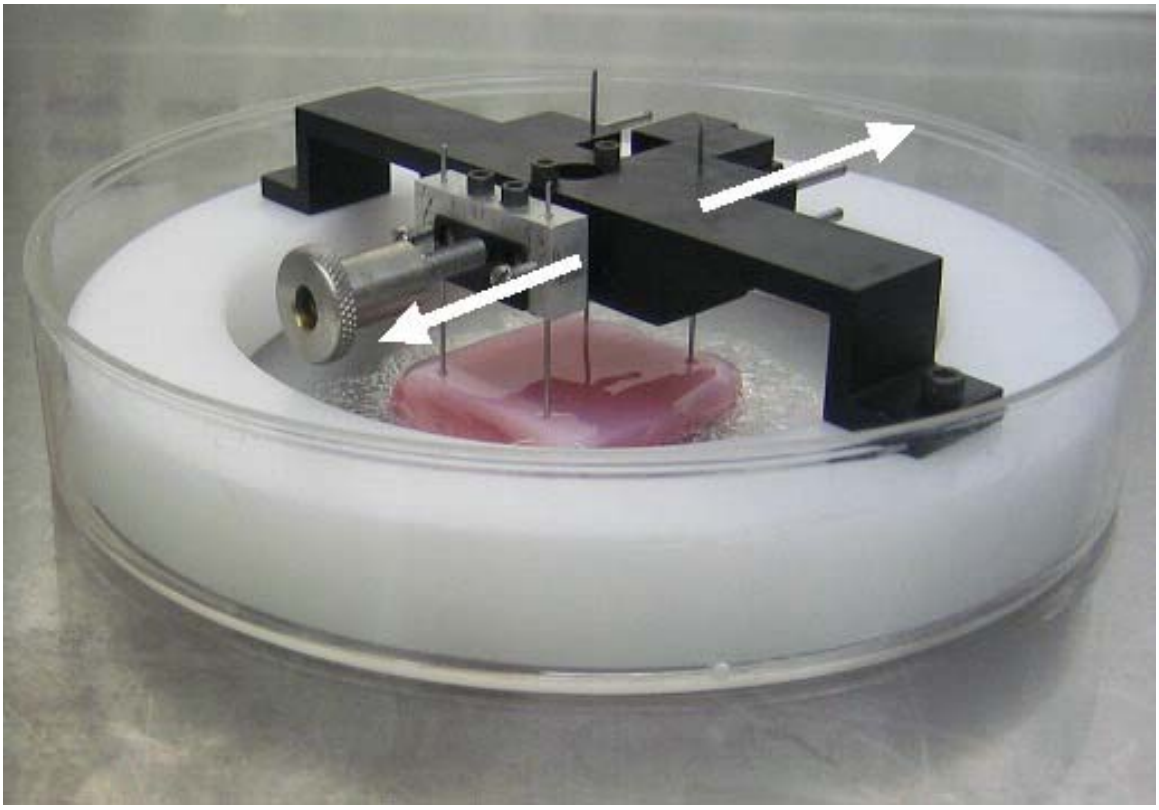

Figure 1. Image of microdistraction model. Note polymerized collagen gel between polyethylene bars and arrows depicting direction of distraction.

Then 0.28 K-wires were placed through the microdistractor into the polyethylene bars. With K-wires running through the distractors into the bars and the bars incorporated into the gels, linear distraction forces applied to the K-wires would be transmitted to the gels and cells within it. The microdistraction device consists of two main parts: the base and the distractor. The base, composed of Delrin, is the anchor for the distraction apparatus and has a central well for the collagen gel. The overlying distractor allows for lengthening (distraction) or shortening (compression) in 0.1mm increments (Parker Hannifin Corporation, Daedal Division, Irwin, PA). All parts of the apparatus are autoclavable and are kept sterile.

Experimental Design

Three study groups were used: 1) distraction, 2) oscillation (distraction and compression) and 3) no force (control) (n=30)(Figure 2). Each gel was prepared as described above. The gels in the distraction group were unstressed for 48 hours (latency). Then, they were distracted 0.5mm every 24 hours for 14 days. Similarly, the gels in the oscillation group were unstressed for 48 hours. On day 3, the oscillation gels were distracted 1mm. On day 4 and day 5, oscillating gels were compressed 1mm/day. Oscillating gels then continued with cycles of distraction, 1.0mm/day every for 2 days, and compression, 1.0mm/day for 2 days so that gels were taken through a neutral position every other day. Cycles of distraction and compression were continued for 14 days. The control gels remained unstressed throughout the duration of the experiment (16 days).

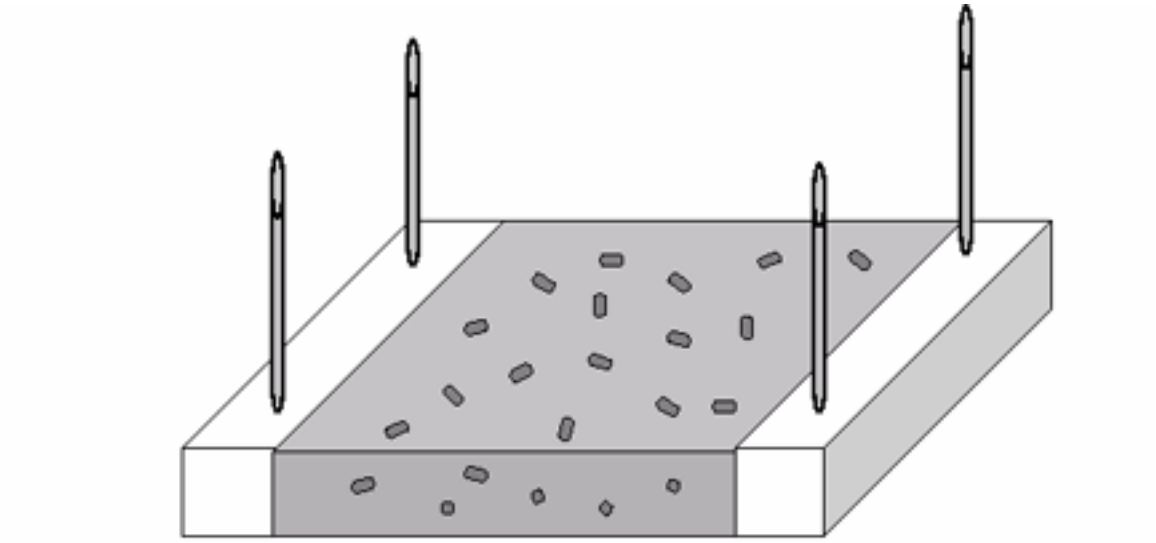

Control (no force) Group

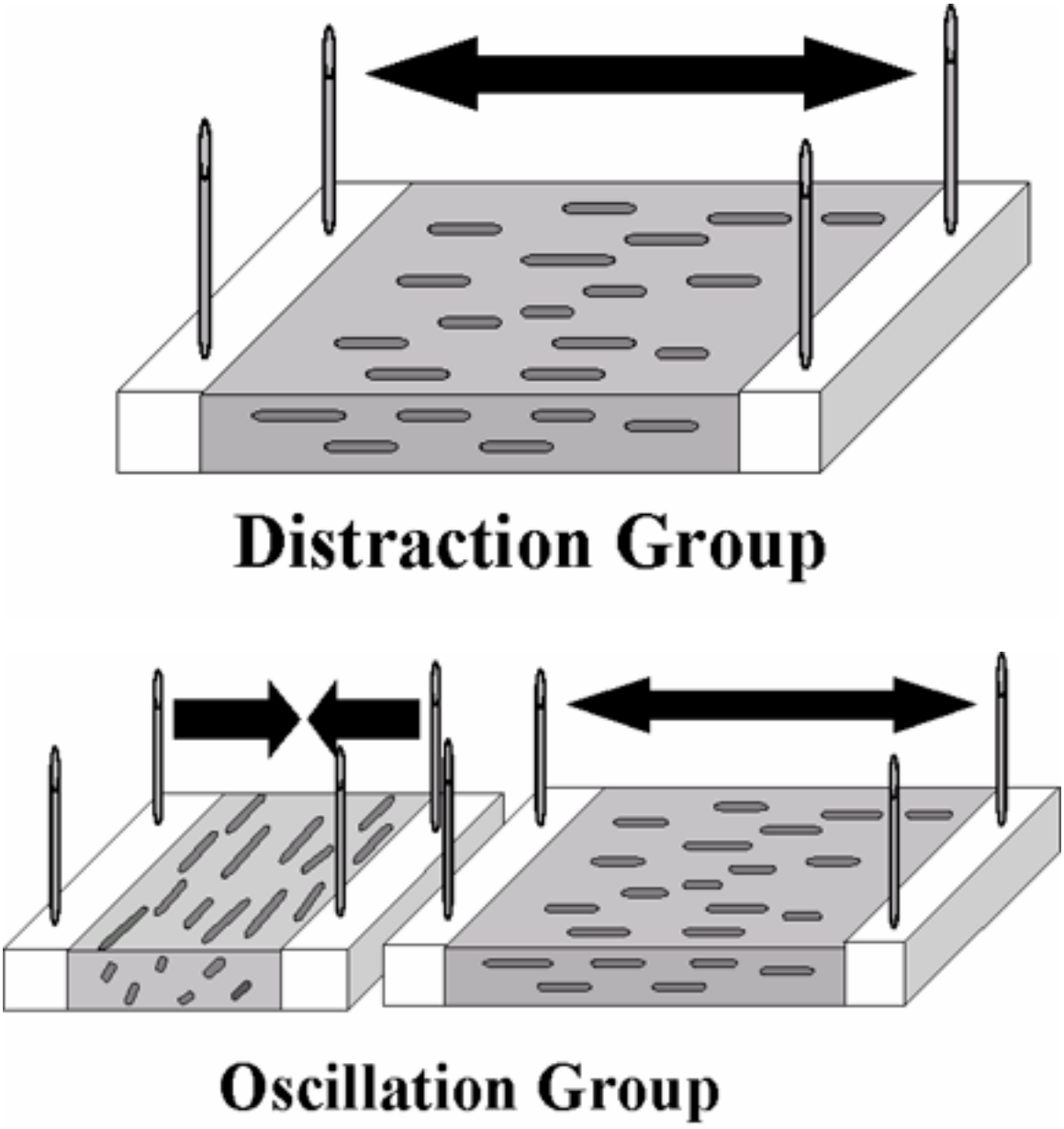

Figure 2. Illustration of 3 experimental groups with MC3T3 cells within the collagen matrix and K-wires placed in peripheral polyethylene bars.

a) Control Group: no stress was applied;
b) Distraction Group: the bars were moved away from each other 0.5mm per day (where arrow depicts vector of linear force);
c) Oscillation Group, stress was applied in an alternating manner:
    i) During period of compression, the bars were moved towards each other (1.0mm per day); and
    ii) During periods of distraction, the bars were moved away from each other (1.0mm per day).

Morphological Analysis

Using an Axiovert 25 microscope (Zeiss™), a Nikon Coolpix 4500 and a23mm eye-piece adaptor (MVIA, Inc, Monaca, PA), images of each gel were taken (100X magnification). Five images in each of four distinct layers of the three dimensional gels were collected per gel daily. For each day a gel had images catalogued as L1 through L4 (four vertical layers) and as image A through E (five horizontal regions) for a total of 20 images. Each gel had 320 images recorded over the course of the 16-day experiment (n=30 or 9600 images). Images were randomly collected by three independent viewers and catalogued. With the proper objective, light microscopy adequately revealed cellular morphology and orientation, negating the necessity for staining of the cells.

KS-300 software (Zeiss™) was used for morphologic analysis. On a cellular level, both the aspect ratio and deviance from the axis of stress were analyzed. The aspect ratio is the largest diameter of the cell divided by the shortest diameter of the cell. This differentiates a cell population that is elongated from one that is more round. The deviance from axis of stress is the absolute difference between the direction of force (distraction or compression) and the angle of cellular orientation (ºdeviance from axis of stress), measured using the following equation:

$$\text{Deviance} = 1 - [(|\text{ºdeviance from axis of stress}|)/90º]$$

Thus, a cell oriented along the line of force (|ºdeviance from axis of stress| = 0º) would have a deviance equal to zero and a cell oriented perpendicular to the force (|ºdeviance from axis of stress| = 90º) would have a deviance equal to one). The interactive measurement function of KS-300 was used to outline the cells with clear boundaries from each of the collected images within different areas and different planes of the gel. To

assure consistency, from the list of measurements, 25 values were randomly selected for each image. An average value was calculated for each image, for each layer, and for each day, for each gel and for each group of gels.

Part I: Validation of Microdistraction Model

Morphologic image analysis was used to compare cells from different locations within the same gel [i.e.- at the same time (day 1, 7, or day 14) and undergoing the same force (distraction, oscillation, or no force)]. Mean aspect ratios of cells in the periphery of the gel were compared to cells in the center of the gel. This comparison was done to determine if cellular response or stress transmitted by the microdistractor varied in different regions of the gel. Thus, cell shape in one layer was compared to cell shape in other layers of the three-dimensional gel. The mean cellular deviance from axis of stress was used to compare cellular orientation in the periphery versus the center. Also, the mean cellular deviance from axis of stress in one layer was compared to that of cells in other layers.

Morphologic image analysis was also used to demonstrate cellular shape and orientation change over time. The mean aspect ratio of cells prior to initiation of force (latency) was compared to that of cells after 1, 7 and 14 days of force (with either distraction, oscillation or no force (control)). In addition, the mean deviance from axis of stress of latent cells was compared to the mean deviance from axis of stress of cells within the same system at 1, 7 and 14 days.

Part II: Comparison of Distraction, Oscillating, and No Forces (Control)

Morphologic image analysis was used to compare cells in the distraction system to cells in the oscillating system and cells within the control system with no force. Mean aspect ratio and axis of deviance of cells at the same time were used for comparison. In addition, values were plotted over time. Statistically, significant changes in morphological parameters of each group were determined by a single-factor repeated measures ANOVA (GB-Stat, v.6.3).

RESULTS

Cells in the collagen gel survived up to 14 days in distracted, oscillation, and no force environments, with no gels having greater than 15% cell death. Cell survival was equal in the central and peripheral regions of the gel. In addition, cell survival was similar in different layers of the gel.

Part I: Validation of Microdistractor Model

Cells in different locations of the gel demonstrated a similar shape (aspect ratio) and orientation (deviation from axis of stress) when the force applied and time within the gel were the same during continuous distraction. Cells in the gel periphery had similar aspect ratio (or elongated shape) to cells in the central portion (Table 1; $p>0.05$). Also, cells in the periphery had similar deviation from axis of stress (or orientation) as cells in the center of the gel ($p>0.05$). In the vertical plane, cells within one layer had similar aspect ratios to cells of another layer($p>0.05$). In addition, cellular deviation from the axis of stress (orientation) did not vary in the different layers of the gel (top, middle, or bottom) ($p>0.05$). For example, cells at the top layer, L-1, had a mean aspect ratio of 5.1

$\pm$ 0.2 at day 7 of distraction and cells at the bottom layer, L-4, had a mean aspect ratio of 5.0 $\pm$ 0.4 at day 7 of continuous distraction ($p>0.05$).

When comparing cellular morphologic change over time during distraction, there were differences in both aspect ratio (elongation) and deviance from the axis of stress at day 1, day 7, and day 14 (Table 1). Cells were noted to elongate during continuous distraction, with a mean value of 1.1 at day 1; 5.0 at day 7; and 5.5 at day 14 ($p<0.05$). Thus, the cellular morphologic response to the applied force of the microdistractor over 2 weeks was an increase in length compared to width. In addition, cells developed a decrease in the deviation from the axis of stress with a value of 0.50 at day 1; 0.21 at day 7; and 0.16 at day 14 ($p<0.05$). Thus, cells became progressively more oriented toward the axis of the distraction force over time.

Part II: Comparison of distraction, oscillation, and no forces (control)

The distraction group had the greatest elongation of cells, quantified as the aspect ratio (Figure 3). The cells in the distraction group demonstrated a progressively increased aspect ratio for the first week then maintained a steady level (approximately 5.8). With the control and oscillation groups, there was also an initial progressive elongation of cells and increase in aspect ratio. By contrast, both the control and oscillation group had a leveling off at a lower aspect ratio (approximately 26% lower for control group and 17% lower for the oscillation group).

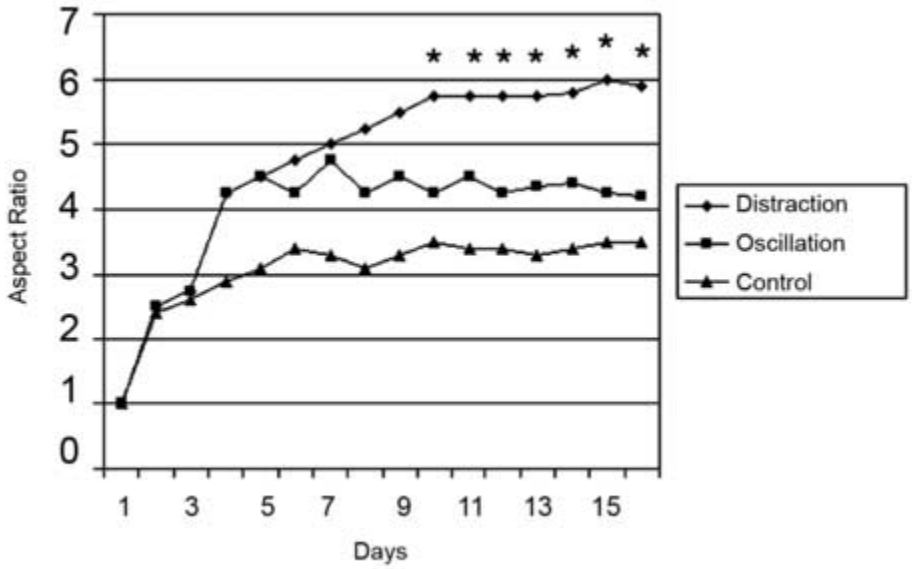

Figure 3. Aspect Ratio (Averaged value for groups examined)
The distraction group demonstrated the greatest elongation of cells, quantified as the aspect ratio. In the control and oscillation groups, there was also an initial progressive elongation of cells and increase in aspect ratio. By contrast, both the control and oscillation group had a leveling off at a lower aspect ratio (approximately 26% lower for control group and 17% lower for the oscillation group).

With regard to the orientation of cells, cells appeared to align along the direction of the distraction vector when a linear or distraction force was applied (Figure 4a). Thus, cells in the distraction group had the least deviance from the axis of stress when compared to both the control and oscillation (during compression) groups. Qualitative measurements of the deviance from the axis of stress in the distraction group decreased from the starting point of about 0.5 to a value around 0.1 ($p<0.05$). This value was maintained over the course of the experiment.

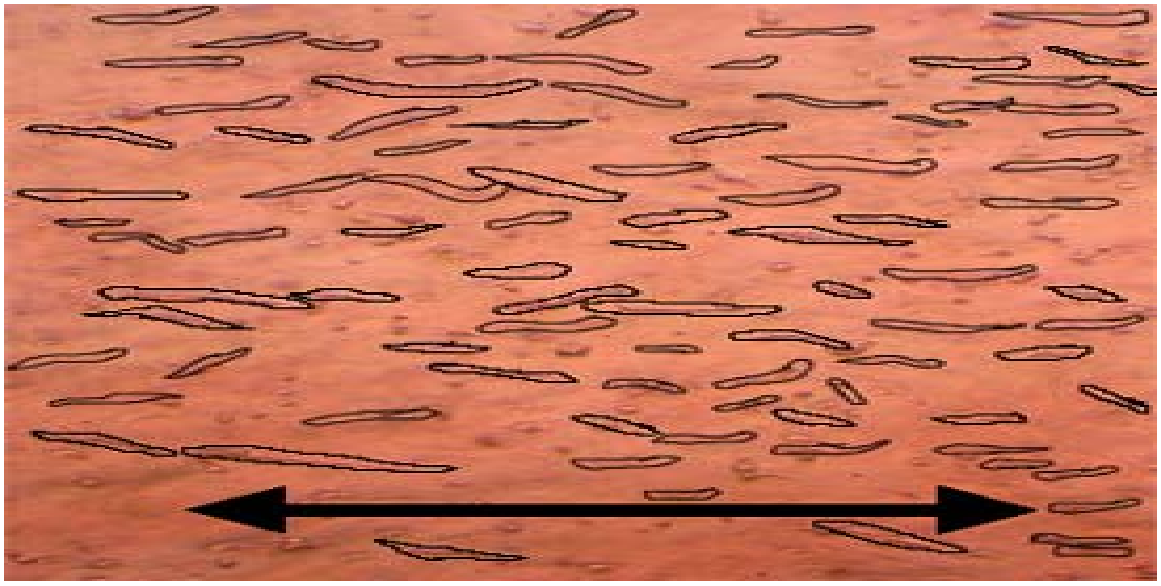

Figure 4a. Light microscopic image (100X) of cells within gel with outlined cell border (day 14). Distraction Group: cells aligned along the axis of force.

In comparison, those cells in the control gel (where mechanical forces were absent), remained at this starting point throughout the course of the experiment (Figure 5). Their random orientation was consistently noted at each time point as shown in the representative image (Figure 4b).

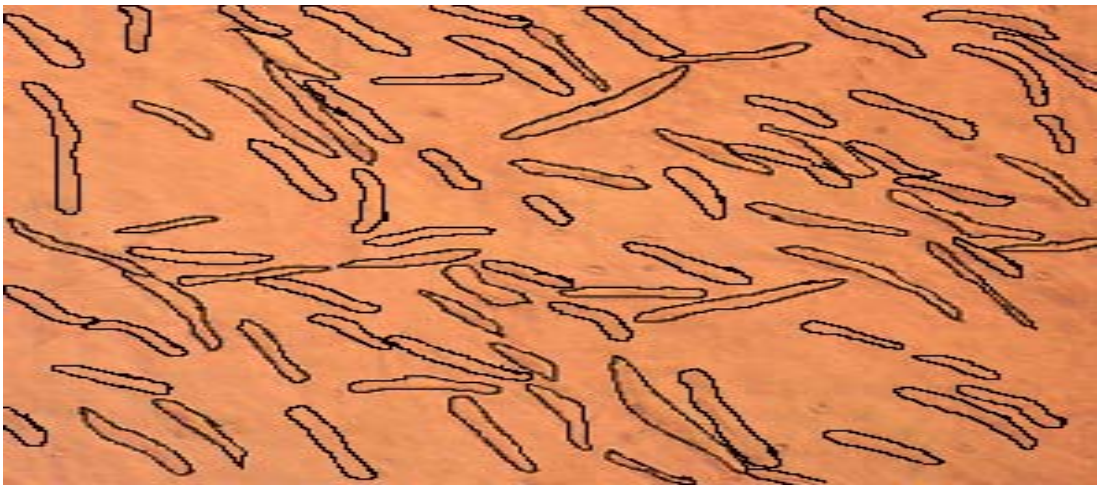

Figure 4b. Light microscopic image (100X) of cells within gel with outlined cell border (day 14). Control Group: cells are randomly oriented;

However, with oscillation forces, this random orientation was not seen. During periods of compression, the cells reached values of 0.7 and during the distraction phase, the cells decreased to values closer to 0.4, which were values significantly different than both controls or each other ($p<0.05$). In other words, a cyclic pattern in the deviance from the axis was noted. The oscillation cells switched their orientation from near alignment (to the distraction force) to perpendicular alignment (to the compression force)(Figure 4c). In Table 1, this switch is depicted as a "zig-zag" line.

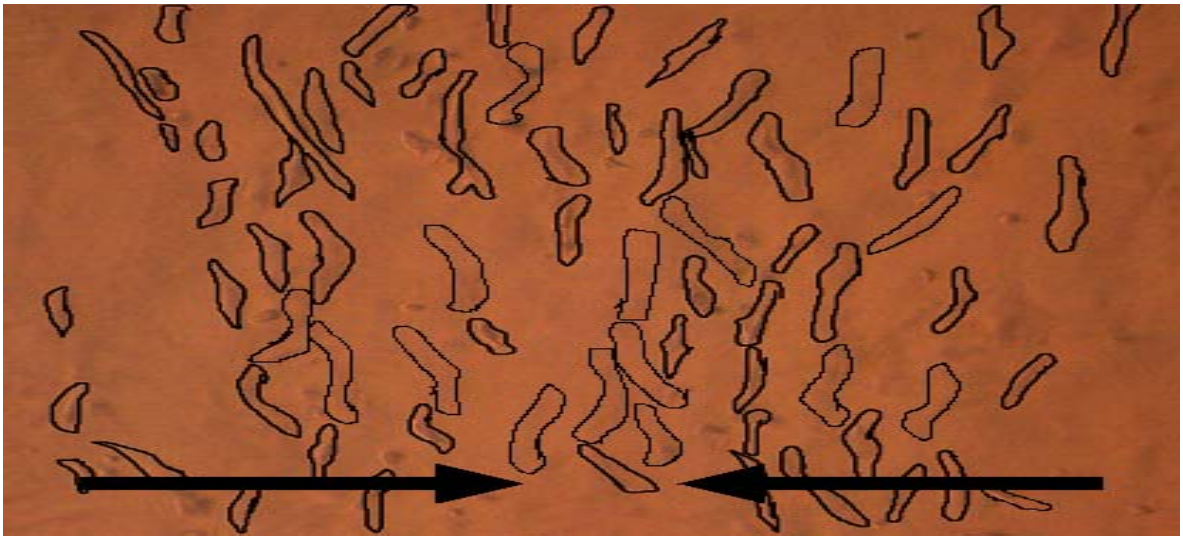

Figure 4. Light microscopic image (100X) of cells within gel with outlined cell border (day 14). Oscillation Group: During period of compression, the cells were perpendicular to the axis of force (as shown). During the distraction phase, the cells oriented along the axis of force (see figure 4a).

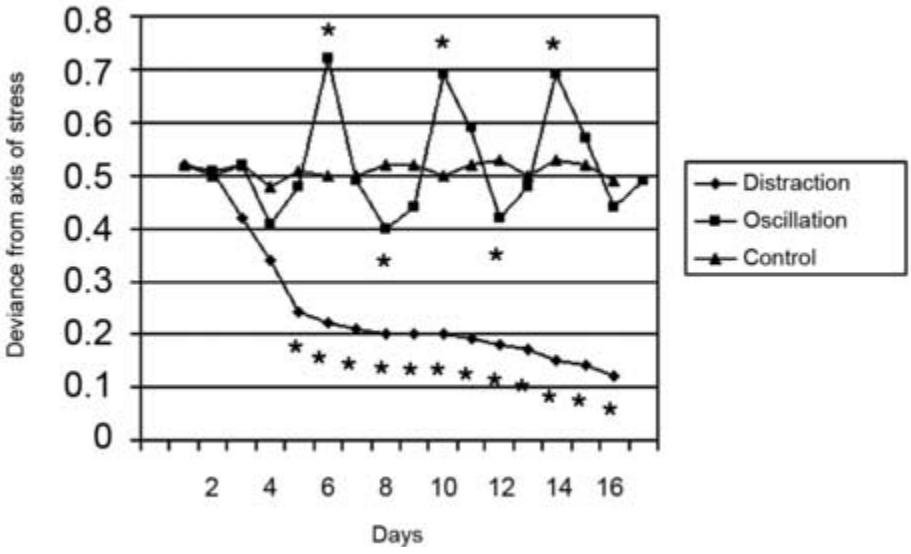

Figure 5. Deviance from axis of stress (cell orientation) during microdistraction.
In the distraction group, the decrease in deviance from axis of stress over time was due to the progressive alignment of cellular orientation with the axis of stress. The control group had a deviance of approximately 0.5, or random orientation of cells. The oscillating group had a zig-zag pattern where, during distraction, a decrease in deviance (with greater orientation towards the axis of stress) occurred and during compression, an increase in deviance (with a perpendicular orientation from the axis of stress) occurred.

Table 1. Cellular morphology during *in vitro* microdistraction

	Aspect Ratio (elongation)				Deviation from axis of stress (orientation)			
	Day 1	Day 7	Day 14	P -value	Day 1	Day 7	Day14	P -value
Periphery	1.1±0.1	5.0±0.3	5.4±3.0	< 0.05	0.48±0.04	0.21±0.03	0.16±0.02	< 0.05
Center	1.0±0.2	4.8±0.4	5.7±3.0	< 0.05	0.50±0.03	0.19±0.02	0.17±0.03	< 0.05
L-1	0.9±0.2	5.1±0.2	5.6±4.0	< 0.05	0.51±0.04	0.24±0.02	0.15±0.02	< 0.05
L-2	1.2±0.1	4.9±0.3	5.3±3.0	< 0.05	0.53±0.03	0.23±0.03	0.13±0.02	< 0.05
L-3	1.0±0.2	5.3±0.3	5.9±3.0	< 0.05	0.49±0.03	0.18±0.02	0.18±0.03	< 0.05
L-4	1.1±0.2	5.0±0.4	5.5±4.0	< 0.05	0.50±0.03	0.22±0.02	0.14±0.02	< 0.05
p - value	> 0.05	> 0.05	> 0.05		> 0.05	> 0.05	> 0.05	

1. Cells in <u>different locations</u> of the gels during distraction, either in the periphery or the center or within different vertical layers (L-1 to L-4) had similar mean aspect ratios and similar deviation from axis of stress. Note the similar values in the columns ($p>0.05$).

2. Cellular shape and orientation <u>changed over time</u>. This was demonstrated by difference in aspect ratio (elongation) at day 1, day 7 and day 14 of distraction and the difference in deviance from the axis of stress at day 1, day 7, and day 14 of distraction. Note the different values in the rows ($p<0.05$).

DISCUSSION

Ilizarov's concept of distraction osteogenesis is based on the Law of Tension-Stress: tissues subjected to slow steady traction become metabolically activated and maintain active growth and regeneration.[97] In addition to bone lengthening without grafting, DOG allows for the repair of extensive defects of bone, nerves, vessels, and soft tissues.[98] A surgical osteotomy, placed in nearly any anatomic location, has the regenerative capacity of a growth plate when controlled distraction pulls apart the bony edges. New bone will form at the site of the osteotomy. The distraction process has been adapted to the craniofacial skeleton and has become a widely accepted modality in the correction of craniofacial anomalies. Under optimal conditions, this neo-osteogenesis resembles intramembraneous bone formation with no cartilaginous intermediate. In

response to mechanical loading, cells organize and relate to one another. Similarly it is hypothesized that if such a stress is applied *in utero* across the calvarial sutures bone growth may be induced. If such bone growth occurs in an unregulated fashion craniosynostosis may result.

Animal studies of distraction osteogenesis have focused on optimizing the latency (time of initiation), rate (length per day), rhythm (activations per day), and length of distraction. Histologic analyses of the osteotomy site have identified distinct zones within the regenerate during lengthening and healing.[99]

In vitro studies of distraction have used models that stress cells. The Flexercell unit (Flexercell Corp., McKeesport, PA) is a computer-based system that uses a vacuum to apply traction to a monolayer of cells.[86-93] Limitations of this system include: 1) an uneven distribution of stress and 2) lack of cell contact on a three-dimensional level. Cells within a Flexercell unit that are near the center of the well are subjected to less force (are stretched less) than those near the well edges. In addition, the arrangement of cells in a monolayer eliminates the interaction of the cells with their surrounding three-dimensional environment normally present *in vivo.* The cost of the unit may also limit its use.

Distraction osteogenesis in an organ culture system has been described, but has not yet been used to study the cellular mechanisms.[100] Choi et al have used scanning electron microscopy to examine the spatial and temporal features of proliferating vessels during distraction osteogenesis but few studies have looked specifically at cellular morphology of pre-osteoblasts during distraction.[101] As an alternative *in vitro* system, we developed a microdistractor. Our model was adopted from a series of studies looking at

isotonic biaxial loading of fibroblasts in collagen gels. Knezevic et al. designed a loading system in which weights suspended off polyethylene bars resisted the contracture of a collagen gel.[95]

Our microdistraction model allowed cells to be seeded evenly throughout the 3-D gel. Cells were easily visualized by light microscopy to assess morphologic change as a response to stress. Our data showed that morphologic changes (in elongation and in orientation) were consistent throughout the gel in both the center and periphery and in different vertical layers. This suggested that the force was evenly applied to all cells in the gel. In addition, when linear distraction forces were applied, a morphologic change (in elongation and in orientation) occurred over time, suggesting a morphologic response to the applied stress.

Our model showed that with different forces applied (distraction, oscillation, or no force) different morphologic changes (in shape and in orientation) occurred over time. In all groups, elongation of cells occurred during the first week suggesting similar adjustment of cells to the 3-D environment. The linear distraction force then caused the most elongation of cells.

Morphologic data also suggested that cellular orientation was sensitive to the direction of force and the type of force (distraction verses compression). In the oscillating group, orientation of cells "flip-flopped" from parallel to perpendicular orientation when distraction force was switched to compression. The term "pumping the regenerate" has been used to describe a clinical method of alternatively distracting and compressing the distraction gap to promote healing.[102] In our *in vitro* system, this method resulted in morphologic changes which may be considered favorable for cellular

interaction and bone healing.

Extensive research has shed light on the importance of mechanical stress and resultant cellular deformation through stretching or compression in such processes as osteogenesis, proliferation, apoptosis, etc..[103-110] In this study, we have shown that the microdistractor system allows for more accurate study of these processes because it induces a unique and reproducible pattern of cellular morphology change that is constant throughout the gel system being tested. The microdistractor is a valuable system for the study of stress on an *in vitro* cellular population. In the subsequent chapter (Chapter 4) this system is used to apply uniform stress to pre-osteoblasts. The gene expression patterns for genes of osteodifferentiation are documented. In doing so it is demonstrated that stress induces osteodifferentiation and thus may play a role if applied during development when cellular potential is greater.

CHAPTER 4
PRE-OSTEOBLASTS OSTEODIFFERENTIATE TO STRESS

Introduction: The biology of osteoblasts is influenced by: 1) an environment that is constantly subject to compressive and tensile forces and 2) a complex three-dimensional extracellular matrix throughout which the cells are dispersed and interact with each other. To study in vitro changes to osteoblasts, we have chosen to use a microdistraction model. This model permits the application of uniform linear stress on three dimensional collagen gel seeded with cells.

Methods: Collagen gels seeded with cells from an immortalized preosteoblast cell line (MC3T3-E1) were subjected to distraction, oscillation (alternating cycles of distraction and compression) and no force (control) for a period of 16 days. To evaluate cellular proliferation in response to linear stress, gels were analyzed for cell count and protein concentration. To evaluate cellular differentiation, alkaline phosphatase activity assay and real time PCR analysis of osteogenic markers (osteopontin, osteocalcin, alkaline phosphatase) were performed.

Results:
Proliferation. On the 16^{th} day, the distraction group had the greatest increase in cell count and protein concentration (2.1 and 3.07 fold respectively) when compared to control (1.37 and 2.38 fold) and oscillation groups (1.38 and 2.43 fold respectively).
Differentiation. The oscillation group had an early rise in alkaline phosphatase activity and gene expression (day 2) which plateaued by day 12 (10.5 fold increase in alkaline phosphatase activity on day 12). The distraction group had a later rise in activity and also plateaued (11.5 fold increase in activity on day 14). The control group had a late and gradual increase in alkaline phosphatase activity and gene expression (4.9 fold increase in alkaline phosphatase activity on day 16). This pattern was mirrored in osteocalcin gene expression, with the oscillation and distraction groups showing significantly greater expression than controls on day 16 (1.96 and 1.30 fold, respectively, $p<0.05$). Gene expression of osteopontin was relatively unchanged throughout the study, and was not significantly different among any of the groups.

Conclusion: The Microdistractor system is an effective *in vitro* model for the study of cellular mechanobiology. MC3T3 cells undergoing linear distraction experienced rapid proliferation with a delayed expression of markers of osteogenic differentiation; whereas, cells undergoing oscillation had a rapid expression of osteogenic markers, but a cellular proliferation pattern indistinguishable from that of unstressed controls.

INTRODUCTION

Bone is a dynamic structure that is described by Wolff's law as being responsive in form and function to mechanical stress.[111-114] The biology of osteoblasts is influenced by: 1) an environment that is constantly subject to compressive and tensile forces and 2) a complex three-dimensional extracellular matrix throughout which the cells are dispersed and interact with each other. Clinically, these influences are relevant in reparative processes such as bony fracture healing and distraction osteogenesis.

Most *in vitro* studies of osteoblast mechanobiology have in the past focused on a two-dimensional, monolayer surface, limiting them in two aspects: 1) stress applied to cells is not uniform (cells in different locations of the testing device receive different force) and 2) cells in a two-dimensional monolayer express a different phenotype to cells in a three-dimensional *in vivo* environment.[115-123] To study in vitro changes to osteoblasts, we have chosen to use a microdistraction model. This model, borrowed from the clinical technique of distraction osteogenesis, allows for the application of linear stress to cells and results in consistent cell shape and orientation change.[124] (Figure 1).

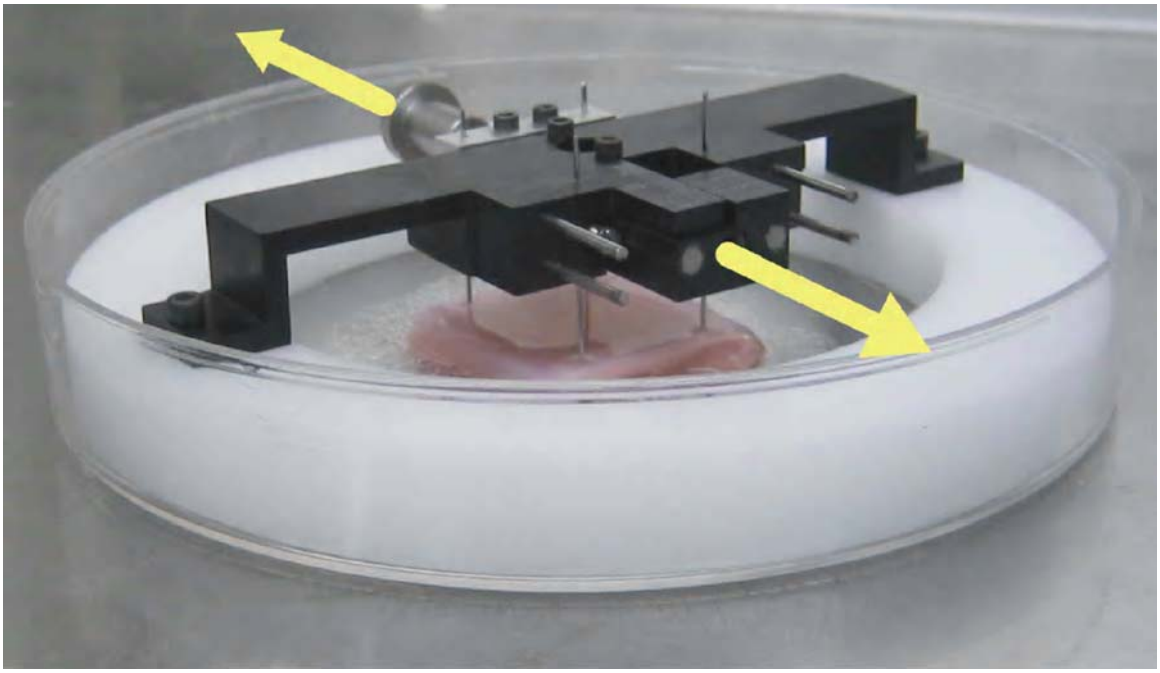

Figure 1. The Microdistractor device with gel in place. Arrows indicate the vector of movement.

The application of uniformly oriented stress is more similar to that normally experienced by osteoblasts *in vivo*. By more closely mimicking the three dimensional microenvironment of bone, this system affords more similar cell-cell and cell-matrix interactions to those observed *in vivo* than in a two dimensional system.[115-123] Furthermore, the microdistractor is inexpensive, re-usable and does not require specialized machinery or software to operate.

Initial research using the microdistraction system (Chapter 3) revealed that there is a distinct and consistent response of cellular morphology to linear stress. Cells took on an elongated shape in a direction parallel to the vector of tension when being distracted, and perpendicular to the vector during the compression phase of oscillation. Importantly,

this cellular morphological response was present in a uniform pattern throughout the collagen gel.[124]

This present study uses the microdistraction model to evaluate the effects of linear stress on the proliferation and differentiation of preosteoblasts *in vitro*. Collagen gels seeded with cells from an immortalized preosteoblast cell line (MC3T3-E1) were subjected to distraction, oscillation (alternating cycles of distraction and compression) and no force (control) (Figure 2). To evaluate cellular proliferation in response to linear stress, gels were analyzed for cell count and protein concentration. To evaluate cellular differentiation, alkaline phosphatase activity assay and real time PCR analysis of osteogenic markers (osteopontin, osteocalcin, alkaline phosphatase) were performed.[125-130]

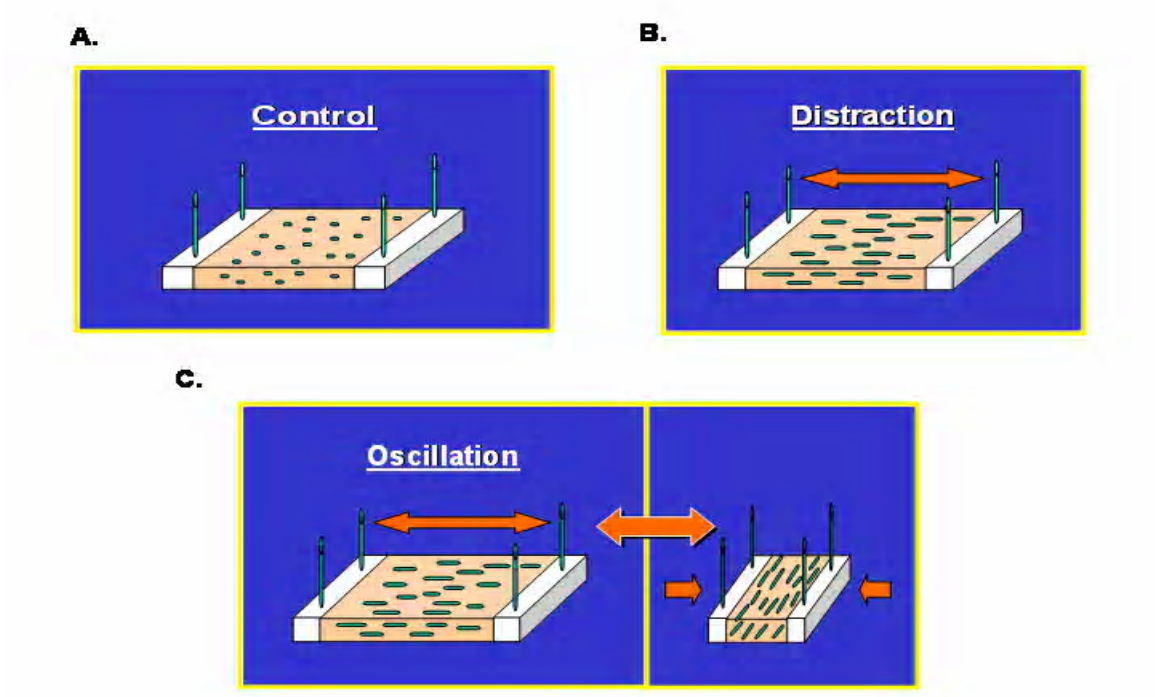

Figure 2. Experimental groups. A. Control (no stress applied to gels). B. Distraction (daily lengthening of gels) C. Oscillation (Cycles of distraction and compression).

MATERIALS AND METHODS

Cell isolation and culture

Mouse osteoprogenitor calvarial cells (MC3T3-E1: clone 4: ATCC, Manasses, VA) were raised in Control medium (CM) containing Dulbecco's modified eagle's medium (DMEM: Sigma, St. Louis, MO), 10% fetal bovine serum (FBS, Summit Biotechnology, Ft. Collins, CO), penicillin (100U/ml: Invitrogen, Grand, Island, NY), and streptomycin (100ug/ml: Invitrogen). Confluent cell cultures were split using 0.25% trypsin-EDTA (Mediatech, Herndon, VA). The cells were harvested between passages 18 through 28.

Preparation of collagen gels

Delrin molds (McMaster Carr Supply Company, Los Angeles, CA) was created to allow the liquid collagen to polymerize into a three dimensional shape (3.5cm x 3.5cm x 1.3cm). The sterile molds were housed in large petri dishes (150 mm X 15 mm) and the edges sealed with silicone stopcock grease (Dow Corning, Midland, MI). Prior to gel preparation, petri dishes were blocked with 2g/ml bovine serum albumin (BSA, EM Science: Gibbstown, NJ) for 1 hr at 37^0C and rinsed with sterile 1x phosphor-buffered saline (PBS).

35mm x 5mm x 3mm Polyethylene bars (Fisher Scientific, Fairlawn, NJ) were pretreated for 96 hours in sulfuric acid. The sulfuric acid was then dialyzed out with distilled water, with changes every 24 hours for 48 hours. The treated polyethylene bars were then placed at either end of the mold (Figure 1).

Gel preparation utilized 8.5ml of cold monomeric Vitrogen 100 (bovine skin collagen, 3.0 mg/ml, Collagen Biomaterials, Palo Alto, CA) mixed with 750µl of 10X Minimum Essential Medium (MEM: Life Technologies, Rockville, MD), 750µl of HEPES at ph 9.0 (Sigma) at 4^{o}C. Optimization of Vitrogen concentration was attained through manufacturer input, information from a collaborating author, and from previous experiments (Askari, et al). MC3T3 cells were harvested from cell culture with trypsin-EDTA, pelleted at 250g for 5 minutes, washed in PBS and resuspended in DMEM at a concentration of 4x10^{6} cells/ml. 500ul of the suspended cell solution were mixed with the Vitrogen solution at 4^{o}C. Five milliliters of the Vitrogen/cell suspension was poured into a mold and was allowed to polymerize for 1 hour at 37^{0}C. The resulting gels contained approximately 1x10^{6} cells (2x10^{5} cells/ml). Subsequently, the seeded gels were maintained in control media.

Microdistractor Design

After gel polymerization, the delrin molds were removed and the microdistractor devices were placed within the large petri dish over the collagen gel (Figure 1). 0.28 inch Kirshner-wires (K-Wires) (De Puy Orthopedics, Warsaw, IN) were placed through the microdistractor into the polyethylene bars. The resultant continuous distraction-gel system transmits linear distraction forces applied by the microdistractor via the K-wires to the gels and cells within it.

Each microdistraction device consists of two main parts: the base and the distractor. The base, composed of delrin, is the anchor for the distraction apparatus and has a central well for the collagen gel. The overlying distractor allows for lengthening (distraction) or shortening (compression) in 0.1mm increments (Parker Hannifin

Corporation, Daedal Division, Irwin, PA). All parts of the apparatus are autoclavable and are kept sterile.

Cell Harvest Procedure

Immediately after gel polymerization, and on days 2, 4, 6, 8, 10, 12, 14 and 16, gels from each group were immersed separately in 3ml of 450 U/ml collagenase type IV (Worthington Biochemical Corporation, Lakewood, NJ). The digested cell suspension was centrifuged at 200g for 5 minutes, washed with PBS, centrifuged again and re-suspended in 1 ml of PBS. The final cell solution was used for proliferation and differentiation assays. A total of 3 gels from each group were digested.

Experimental Design

Three experimental groups were studied: 1) distraction, 2) oscillation (distraction and compression) and 3) no force (control) (n=30) (Table 1, Figure 2). Each gel was prepared as described above and maintained in osteogenic media [CM supplemented with 0.1μM dexamethasone, 50μM ascorbate-2-phosphate and 10mM β-glycerol phosphate (Sigma)]. The gels in the distraction group remained unstressed for 48 hours (latency) followed by a 0.5mm distraction every 24 hours for an additional 14 days.

Table 1. Experimental Design.

Day	Control (n=30 gels)	Distraction	Oscillation	Distance Advanced or Compressed (* = Gel at neutral point)
1	0 mm*	0 mm*	0 mm*	
2	0 mm*	0 mm*	0 mm*	
3	0 mm*	+0.5 mm	+1.0 mm	
4	0 mm*	+0.5 mm	-1.0 mm*	
5	0 mm*	+0.5 mm	-1.0 mm	
6	0 mm*	+0.5 mm	+1.0 mm*	
7	0 mm*	+0.5 mm	+1.0 mm	
8	0 mm*	+0.5 mm	-1.0 mm*	
9	0 mm*	+0.5 mm	-1.0 mm	
10	0 mm*	+0.5 mm	+1.0 mm*	
11	0 mm*	+0.5 mm	+1.0 mm	
12	0 mm*	+0.5 mm	-1.0 mm*	
13	0 mm*	+0.5 mm	-1.0 mm	
14	0 mm*	+0.5 mm	+1.0 mm*	
15	0 mm*	+0.5 mm	+1.0 mm	
16	0 mm*	+0.5 mm	-1.0 mm*	
	0 mm	7 mm	0 mm	**Total Distance**

Similarly, the gels in the oscillation group were unstressed for the first 48 hours. On day 3, the oscillation gels were distracted 1mm. On day 4 and day 5, oscillating gels were compressed 1mm/day. Oscillating gels then continued with cycles of distraction, 1.0mm/day every for 2 days, and compression, 1.0mm/day for 2 days so that gels were taken through a neutral position every other day. Cycles of distraction and compression were continued for 14 days. The control gels remained unstressed throughout the duration of the experiment (16 days).

Part I: Proliferation

Cell count

Prior to gel digestion, digital images were taken using an Axiovert 25 microscope (Carl Zeiss, Inc., Thornville, NY), a Nikon Coolpix 4500 camera (Nikon Inc., Melville, NY) and a 23mm eye-piece adaptor (MVIA, Inc, Monaca, PA) (100X magnification). Five images in each of four distinct layers of the gels were collected daily under 100X magnification. For each day gel images were catalogued as L1 through L4 (four vertical layers) and as image A through E (five horizontal regions) for a total of 20 images. Each gel had 320 images recorded over the course of the 16-day experiment (n=30 or 9600 images). Images were randomly collected by three independent viewers and catalogued.

KS-300 software (Carl Zeiss, Inc., Thornville, NY) was used for morphologic analysis and cell counting. The cell content of each gel for each day analyzed was scored as the sum of all cells in all images obtained from the gel on that day. While this number was not the true cell count for the gel, it gave a standardized value that became a relevant indicator of cellular concentration over the course of the study.

Protein Assay

Total protein concentration was measured using the Micro BCA protein assay reagent kit (Pierce Biotechnology, Inc, Rockford, IL) as a measure of cell content, proliferation and, indirectly, cell number.

For this, the digested cell suspensions were serially diluted. 1ml samples were added to the working reagent and incubated at 37°C for one hour. All samples were measured in a Beckman DU-64 spectrophotometer (Beckman Coulter, Inc, Fullerton, CA) at a wavelength of 562nm.

Part II: Osteogenic Differentiation

Alkaline Phosphatase Assay

Alkaline phosphatase assay buffer was prepared by adding two parts 1.5M 2-amino-2methyl-1-propanol (pH 10.25, Sigma-Aldrich Co., St. Louis, MO) to one part 10mM magnesium chloride (Fisher Scientific, Fairlawn, NJ). In a 96-well plate, 50µl of the collagenized cell suspensions was added to 50µl of alkaline phosphatase buffer and incubated at 37°C for 10 minutes. The reaction was stopped by the addition of 100µl of 1M sodium hydroxide (Sigma-Aldrich Co.) and read at 405 nm. Alkaline phosphatase readings were normalized with respect to total protein concentration. 100µl of six standard p-nitrophenol (Sigma-Aldrich) solutions (0M, 0.66M, 1.33M, 2.66M, 4M and 5.33M) in 1M sodium hydroxide were assayed and used to create a standard curve.

Real Time Polymerase Chain Reaction

Alkaline phosphatase, osteocalcin and osteopontin expression was quantitated in each digested sample at each time point. Murine GAPDH primers and probe (5' JOE and 3' TAMRA) were purchased from Applied Biosystems (Foster City, CA). Total cellular

RNA was prepared from an aliquot of the digested cell suspension using the Qiagen RNEasy Minikit (Qiagen Inc, Valencia, CA). RNA samples were treated with DNAse I (Qiagen) to digest residual genomic DNA. cDNA was prepared from each sample using the TaqMan Gold RT-PCR kit for real-time PCR (Applied Biosystems). Quantitative real-time PCR was performed using this kit according to the manufacturer and an ABI 7700 Prism Sequence Detection system. Primer and probe sequences were designed by the UCLA Sequencing Core Facility and synthesized by BioSource (Camarillo, CA). All probes were designed with a 5' fluorogenic probe 6FAM and a 3' quencher TAMRA. The expression of GAPDH was used to normalize gene expression levels.

Statistical Analysis

For each time point evaluated in each of the study arms (distraction, oscillation or control), the values obtained for each of the three gel in that group were averaged and plotted. An un-paired t-test and one-way ANOVA test (GB-Stat, v.6.3) were performed to determine statistical significance between and among values, respectively. Statistical significance was considered for $p < 0.05$.

RESULTS

Effect of stress on proliferation

Throughout the study time-points, cells in control gels took on a random orientation, whereas cells in the distraction group oriented parallel to the distraction vector (Figure 3).

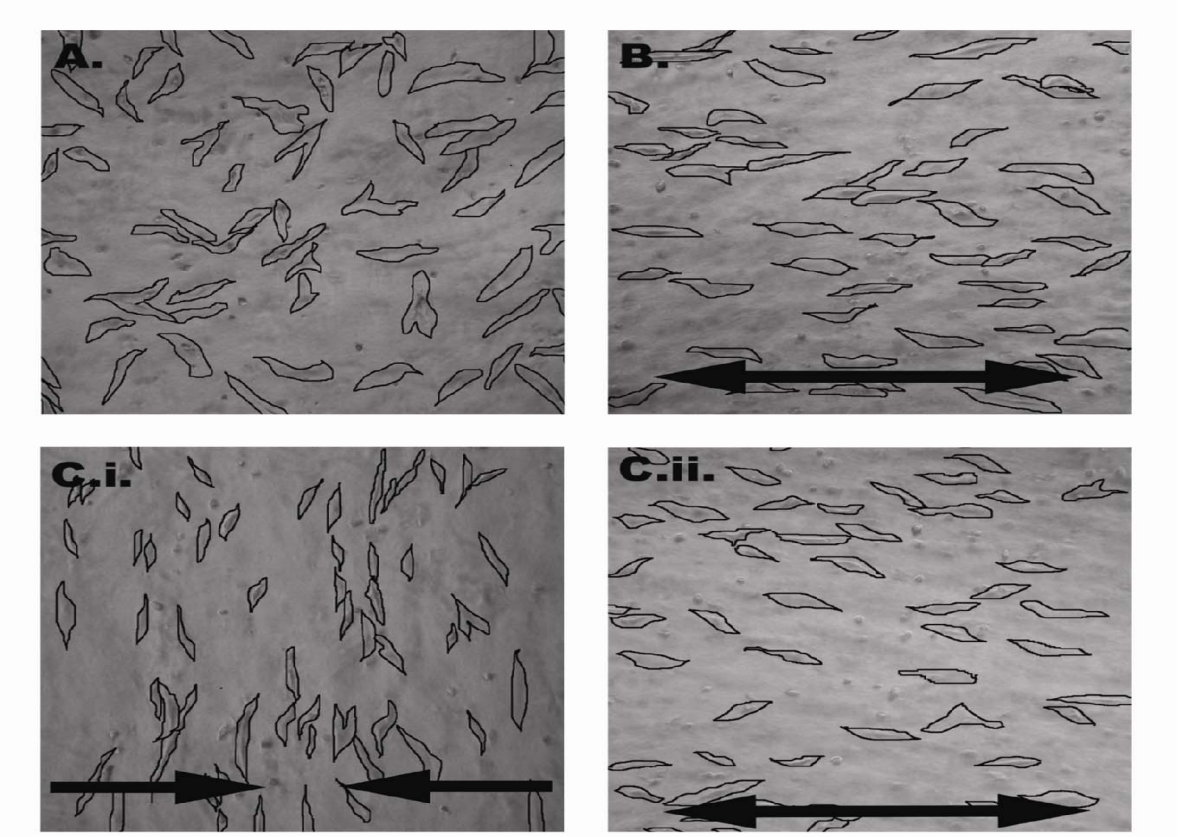

Figure 3. A – Control, **B –** Distraction, **Ci –** Oscillation During Compression, **Cii –** Oscillation During Distraction.

Cells in the oscillation group aligned parallel to the distraction vector when they were being distracted, and aligned perpendicular to the distraction vector when they underwent compression. Over the duration of the study, the control gels demonstrated a gradual, but steady increase in cell number and protein concentration [maximum slope ($\Delta Y/\Delta X$) occurred between days 8 and 10= 39.5 and 17.5, respectively] until the 12th day, after which the rate reached a plateau (Figure 4A &B). On the 16th day, the control gels contained 1.37 fold greater number of cells and had 2.38 fold greater protein concentrations than on day 0 ($p<0.05$). The oscillation group followed a similar pattern [maximum slope occurred between days 8 and 10= 45.5 (cell count) and 19.5 (protein

concentration)], with 1.38 fold greater number of cells and 2.43 fold greater protein concentration on day 16 compared to day 0 ($p<0.05$). These end values were not statistically significant between the control and oscillation groups.

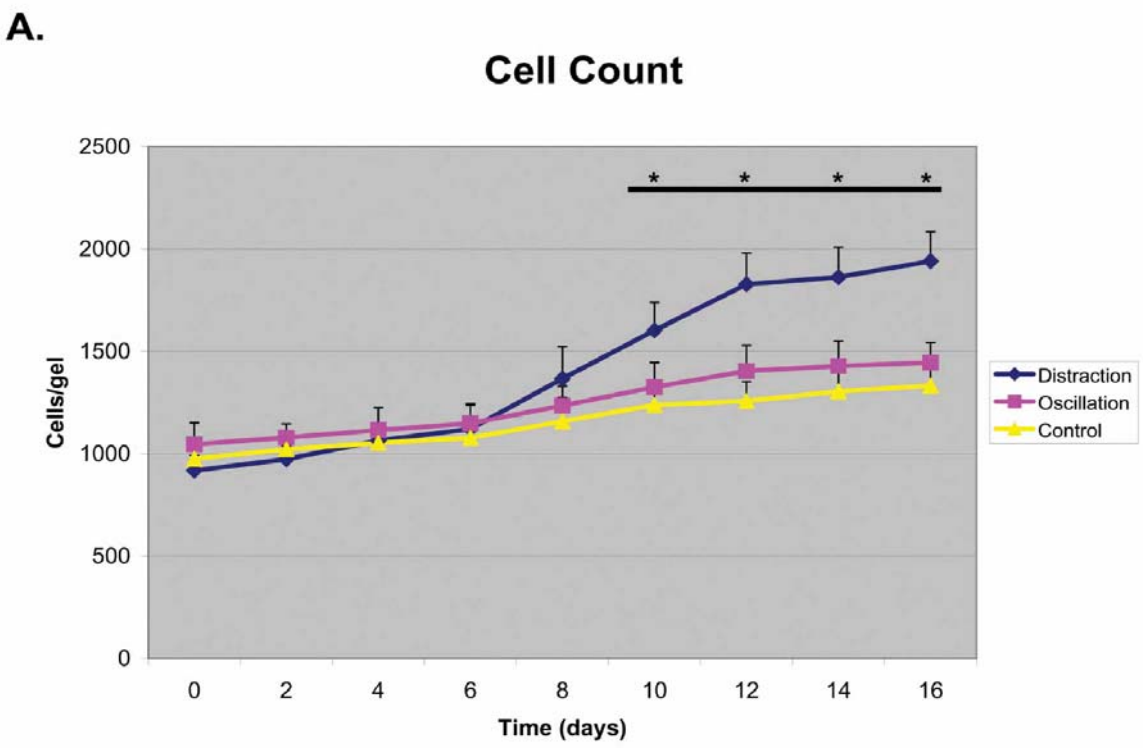

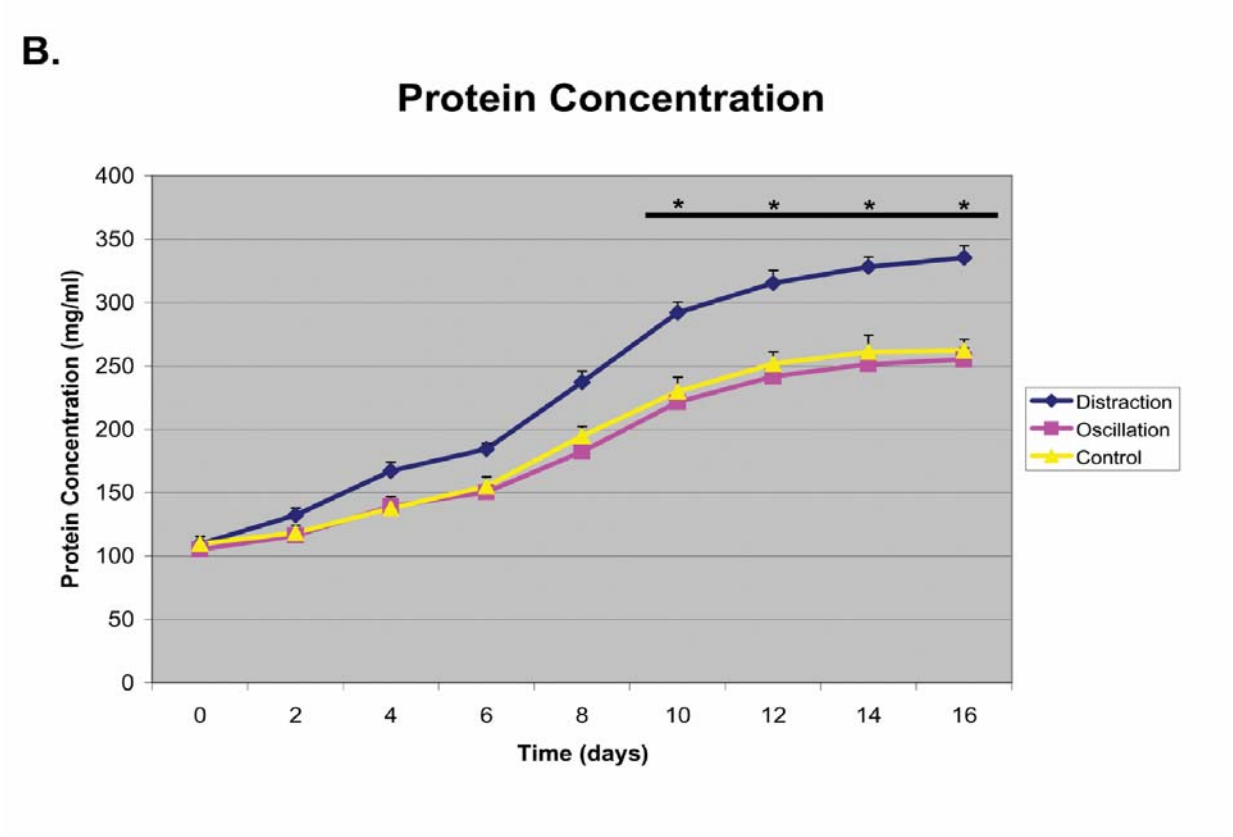

Figure 4. Proliferation profile over time. A. Cell count. B. BCA Protein Assay. *= statistically significant difference ($p<0.05$; $n=3$) between distraction group and control or oscillation group.

The distraction group, however, showed an early and greater total profile of cellular proliferation. This group had an earlier and steeper rise in cell count and protein concentration (maximum slope occurred between days 6 and 8= 122.5 and 26.5, respectively), and as in the other groups, eventually reached a plateau. The cell count was 2.1 fold greater and the protein concentration 3.07 fold greater on day 16 compared to day 0 ($p<0.05$). These values were significantly different from those of the control and oscillation groups. Cell count and protein concentration correlated well with each other.

Effect of stress on differentiation

Control gels had relatively unchanged alkaline phosphatase activity until day 10, after which the activity gradually increased (Figure 5). On day 16, the alkaline phosphatase activity was 4.9 fold greater than that on day 0 ($p<0.05$). The distracted gels also showed an initially slow increase in alkaline phosphatase activity early in the study period; however had a sharp increase in activity on day 10. Alkaline phosphatase activity reached its peak and plateaued on day 14, with activity 11.5 fold greater than that on day 0 ($p<0.05$). Gels undergoing oscillation forces were noted to have an early and rapid rise in alkaline phosphatase activity. A steep rise in alkaline phosphatase activity began on day two, and had reached its peak activity by day 12 (10.5 fold greater than day 0, $p<0.05$) after which it maintained a plateau.

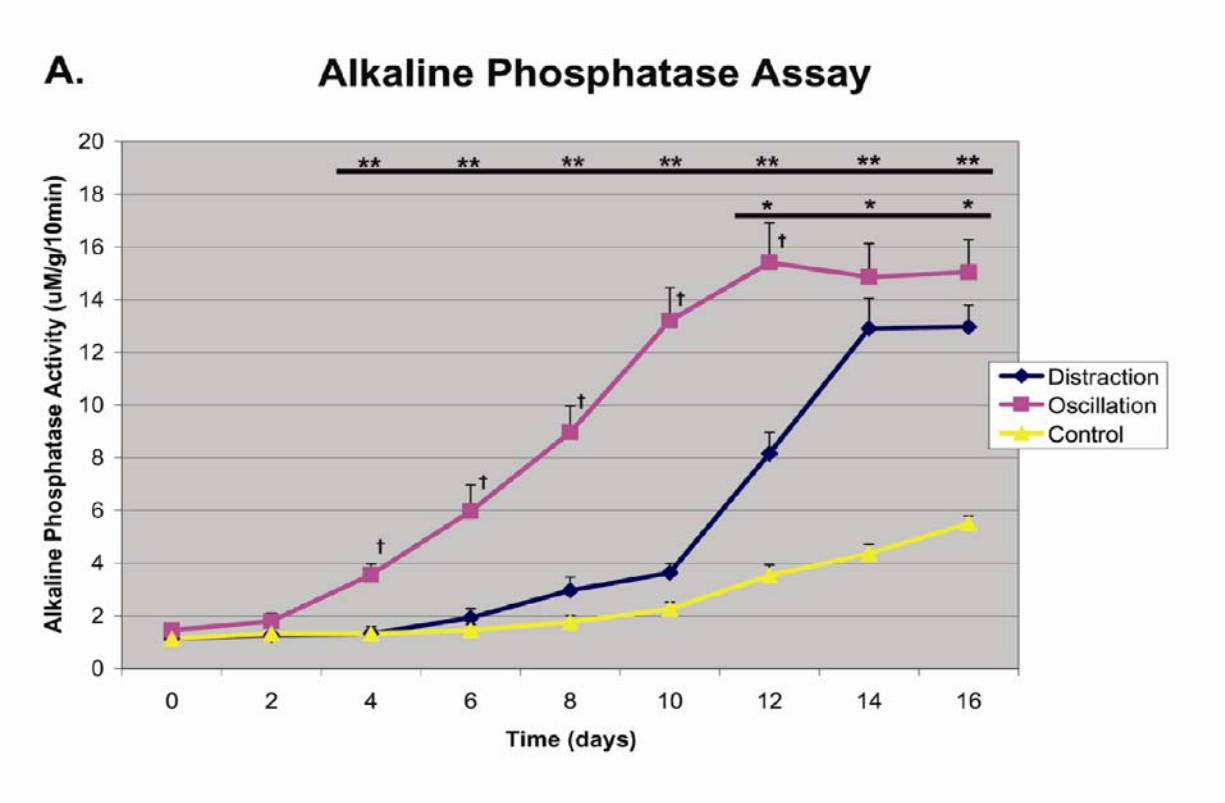

B.

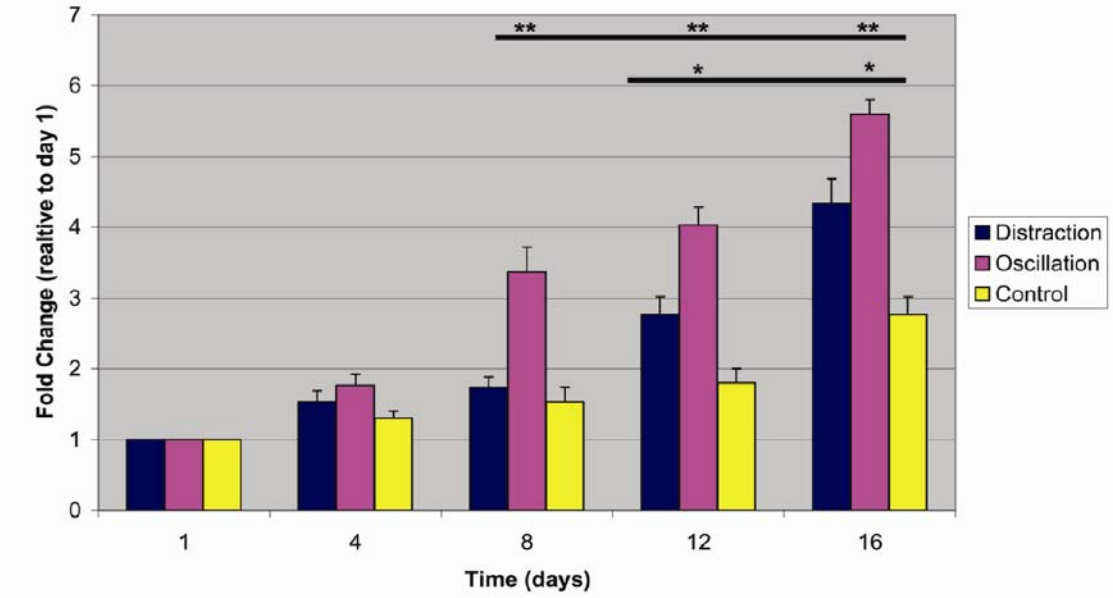
Alkaline Phosphatase Real Time PCR
Fold Change (realtive to day 1)
Time (days)
1
4
8
12
16
0
1
2
3
4
5
6
7
**
**
**
*
*
Distraction
Oscillation
Control

C.

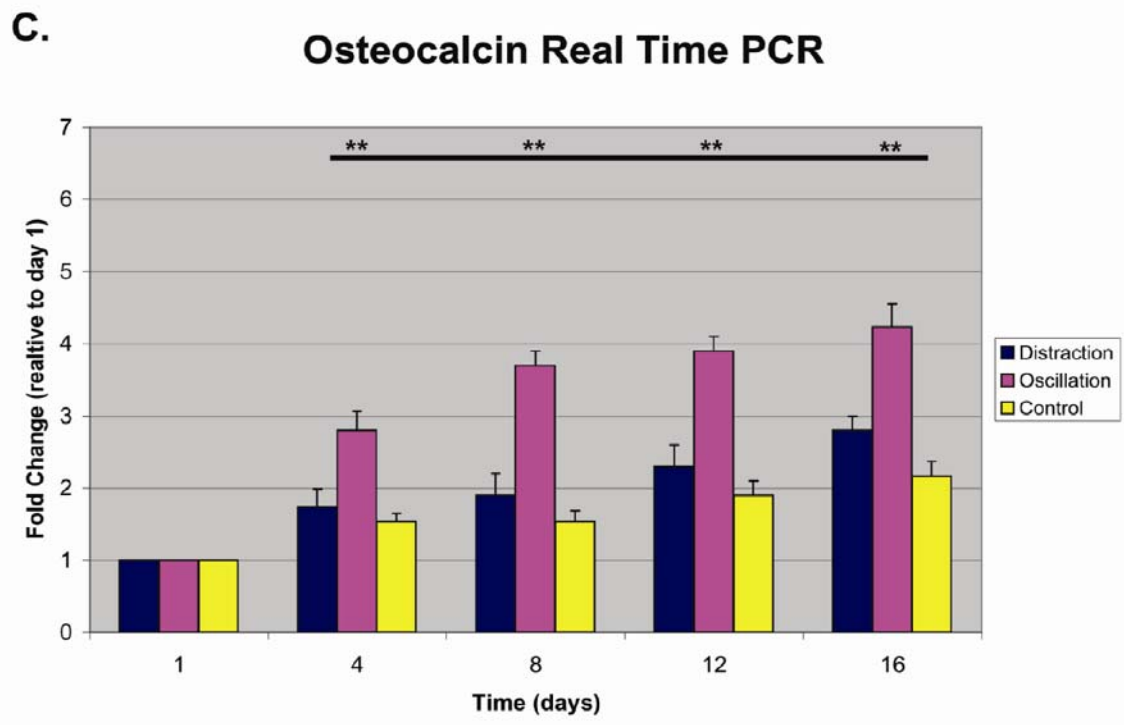
Osteocalcin Real Time PCR
Fold Change (realtive to day 1)
Time (days)
1
4
8
12
16
0
1
2
3
4
5
6
7
**
**
**
**
Distraction
Oscillation
Control

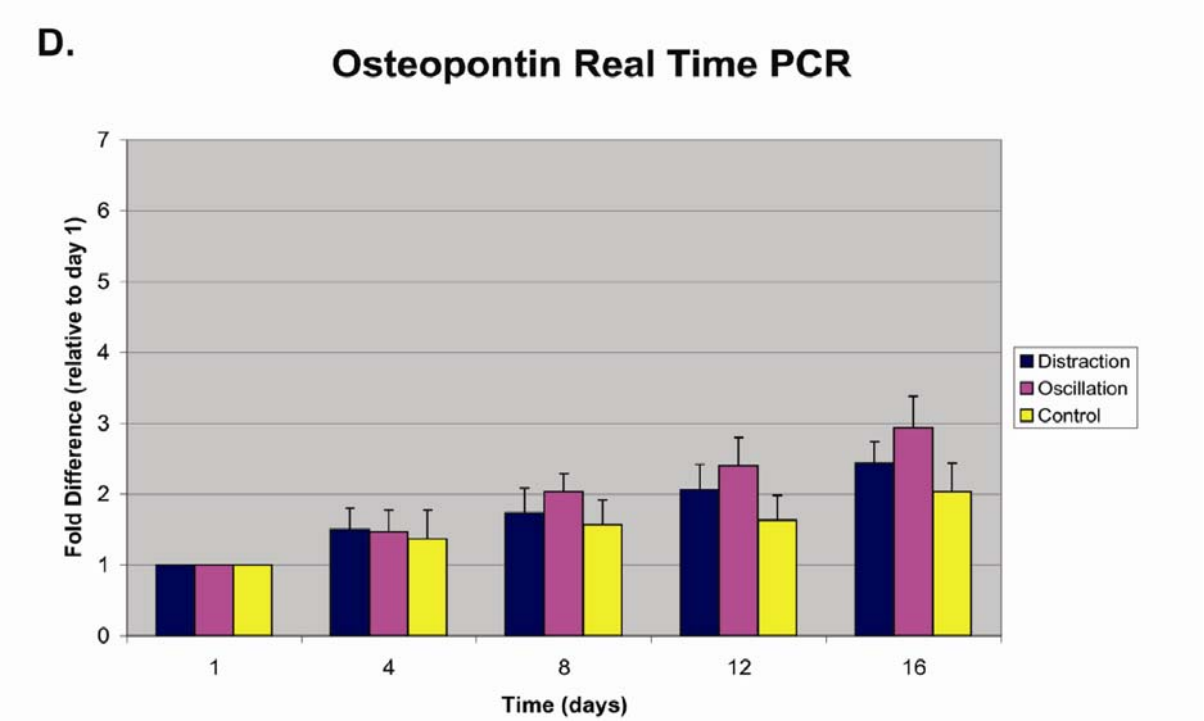

Figure 5. Differentiation profile over time (Real time PCR samples normalized to 28s RNA levels). A. Alkaline phosphatase assay. B. Alkaline phosphatase real time PCR. C. Osteocalcin real time PCR. D. Osteopontin real time PCR. *= statistically significant difference ($p<0.05$; $n=3$) between distraction group and control group. **= statistically significant difference ($p<0.05$; $n=3$) between oscillation group and control group.

Alkaline phosphatase gene expression, as measured by real time PCR, paralleled that of the alkaline phosphatase activity assay. While all groups had an eventual rise in activity, the oscillation group had an earlier and more rapid rate of increase in gene expression relative to the two other groups. This pattern was also seen in osteocalcin gene expression, with an early increase in gene expression of the oscillation group, and late plateau of both oscillation and distraction groups. Both oscillation and distraction groups had greater osteocalcin gene expression compared to controls at the end of the study (1.96 and 1.30 fold, respectively, $p<0.05$). Gene expression of osteopontin was relatively unchanged throughout the study, and was not significantly different among any of the groups.

DISCUSSION

The response of the osteoblast to mechanical stress in a three dimensional system is incompletely understood. This process is critical in normal bone biology, fracture healing and treatment modalities such as distraction osteogenesis. Extensive work investigating osteoblast mechanobiology has shed light on this complicated response, and is beginning to elucidate the cellular and molecular mechanisms of Wolff's Law.

Mechanical stimulation of the osteoblast has been shown to elicit the production of many bone specific markers. Commonly seen is the expression of extracellular matrix proteins including osteonectin, osteopontin, osteocalcin and collagen I as well as intracellular osteogenic associated enzymes such as alkaline phosphatase and CBFA-1.[129-137] In addition to influencing osteogenic differentiation, mechanical stress has been shown to exert a significant effect on cellular proliferation.[133,138-143] Importantly, this research has revealed that osteoblasts respond differently to subtle variations of stress applied to them. Variations of etiology, frequency, duration, and direction of stress as well as substrate composition all have corresponded to differential osteoblast response. Our results demonstrated a profile that shared similarities to previous studies, but revealed some intriguing differences.

Proliferation. Cells in the distraction arm of this study showed an earlier trend towards cellular proliferation, with a rapid increase in cell count and protein concentration and overall greater proliferation compared to the oscillation or control groups. There is a broad relation of this data to previous studies, with many confirmatory, mixed and conflicting reports in the literature. However, few studies have evaluated the specific effect of constant compared to cyclic tension on a cell-seeded in a three dimensional gel.

Akhouayri, et al. noted greater proliferation in cell seeded collagen gels under constant isometric tension compared to those undergoing free contraction or dynamic gels subject to periodic stress.[139] Fong, et al. noted an increase in gene expression of proliferating cell nuclear antigen (a marker of cell proliferation) in a monolayer of rat calvarial osteoblast cells subject to 10% constant equibiaxial strain. However, they did not compare this data to cyclic strain.[136]

In contradistinction, when studying osteosarcoma cells on two-dimensional monolayer, Jiang, et al. found that pulsatile fluid shear flow had a dramatically greater stimulus on proliferation than did constant fluid shear flow.[140] Other studies looking only at the effect of rapid, brief cyclic stress or pulsatile flow have for the most part noted an increase in osteoblast proliferation in response to stress.[133,139,141,143,145] In correlation with our results, a number of studies noted an initial increase in cellular proliferation with subsequent differentiation and expression of osteogenic markers in response to mechanical stress.[137,147]

Differentiation. With regard to the stimulation of osteogenic differentiation by mechanical stress, the microdistractor model revealed two unique patterns for the oscillation and distraction groups. Cells undergoing oscillation had a rapid increase in AP activity and gene expression of AP and osteocalcin with an eventual plateau, whereas cells undergoing distraction had delayed onset of osteogenic differentiation. The literature is most variable when looking at the effect of mechanical stress on osteoblast gene expression, again, with confirmatory, mixed and conflicting reports.

As with the response to cell proliferation, most studies report responses to the effect of rapid, brief cyclic stress or pulsatile flow rather than constant vs. oscillating

stress. In general, there is an increase in both osteocalcin and AP activity in response to stress.[117,132,133,136,139,142] However, some studies noted conflicting patterns of AP and osteocalcin expression[137] or an inhibitory effect of mechanical stress on AP and/or osteocalcin expression.[134.141,.142] In contrast to our findings, Akhouayri, et al noted a decrease in AP activity among cell seeded gels subject to cyclic force when compared to isometrically tense or freely retracting gels.[139]

Interestingly, none of the groups in this study exhibited a substantial increase in osteopontin expression over the study period. Osteopontin is a mechanoresponsive, early to middle marker of osteogenesis that comprises a large proportion of the bony extracellular matrix.[117,146-149] While there is still discrepancy among reports of the temporal and spatial expression of bone markers involved in the osteogenic response to mechanical stress, the apparent absence of osteopontin upregulation may instead reflect the unique and simple nature of this in vitro model.

Toma et al noted that osteopontin expression is responsive to mechanical strain and postulated that this process may be integrin mediated, and hence dependent on the cellular response to the extracellular matrix composition.[131,134,147,150] It is conceivable that the simple composition of the collagen gel matrix did not appropriately stimulate osteopontin gene expression, yet was able to induce alkaline phosphatase and osteocalcin gene expression. This difference in gene expression may be the result of selective signal transduction pathway activation.

A growing understanding of the complex intracellular signal transduction pathways involved in osteoblast mechanobiology has begun to shed light on the mechanism for the variable response to stress. A given stress initiates different cellular

responses (such as differentiation and proliferation) by activation of multiple parallel and often competing intracellular signal transduction pathways.[143,145] Additionally, different stimuli and forms of stress may potentially activate different pathways, resulting in a dissimilar cellular response profile.[134,143,145] For these reasons, it is very likely that cells exposed to different stresses (for example, continuous vs. oscillating force) may have activation of some similar pathways, but ultimately have unique proliferation and differentiation profiles because of differences in signal transduction.

The wide discrepancies in results noted among reports investigating osteoblast mechanobiology may, in part, be due to the complex synergistic intracellular response. Each model used to transduce mechanical strain is different in nature and can impart different types of stress to the cells being investigated. These subtle differences in mechanical stimulation may result in alternate cell signaling profiles with resultant disparities in cellular response. As in this study, the general cellular response to stress is similar, but rarely exactly the same among different models.

CONCLUSION

The Microdistractor system is an effective *in vitro* model for the study of cellular mechanobiology. MC3T3 cells undergoing linear distraction experienced rapid proliferation with a delayed expression of markers of osteogenic differentiation; whereas, cells undergoing oscillation had a rapid expression of osteogenic markers, but a cellular proliferation pattern indistinguishable from that of unstressed controls.

These findings may help to explain the factors that occur in patients with craniosynostosis. For instance if a constant stress similar to distraction were to be

applied a proliferative response would occur, when the stress is removed or oscillated the proliferated populations of cells may osteodifferentiate and lead to fusion.

In summary, Chapters 1 and 2 demonstrated the genetic similarities between a stressed cranial suture and a craniosynostotic suture. Chapters 3 and 4, described the cellular effects of stress; wherein stress may lead to a strong proliferative effect (distraction) or drive towards osteodifferentiation (oscillation). In total these experimental findings lay to rest the controversy as to whether stress may play a role in craniosynostosis and open very interesting new avenues of clinical application. As already mentioned in the acknowledgments, stress applied to Adipose Derived Stem Cells (ADSC's), enabled us to heal critically sized femoral defects without the use of exogenous growth factors. A phenomenon never before reported. The collaborative effort with Macropore® is already underway.

In the future I would like to define the role of stress in wound healing. In particular I feel that the wound vac creates an atmosphere of surface stress that likely promotes its beneficial effects. If this is indeed the case the subsequent step would be to define the pattern of stress that optimizes wound healing (i.e. fibroblast migration, vasculogenesis, ect..). The approach would be similar that describe by this thesis.

SYNOPSIS

My enthusiasm in Plastic Surgery was initially sparked during a third year elective at Yale University. Under the guidance of John Persing, a neuro- and plastic surgeon, I participated in a tremendous number of craniofacial operations, several of which were performed for correction of craniosynostosis. Among the craniosynostotic patients some were syndromic while others were not. It was this latter group that I found particularly fascinating. My reasoning was that if one could understand the process resulting in premature suture fusion (i.e. aberrant bone formation), one could also understand how to generate bone to fill bony defects. I began my enquiry with a project that was an assessment of intracranial volume (ICV) and cephalic index (CI) among non-syndromic sagittal synostosis patients. This project demonstrated that with increasing age, patients progressively deviated away from the mean values towards higher ICV's and lower CI's. Ergo, this meant that despite a synostosed suture, compensatory bone growth was occurring at other sutures. I now desired to understand the biological basis behind this phenomenon. I hypothesized that these processes were all strain induced. Proving such a hypothesis, however, would require seeking a bench and a hood.

At the conclusion of my third year of medical school, I applied for the Sarnat Craniofacial Surgery Research Fellowship and to the Regenerative Bioengineering and Research (ReBaR) Laboratories, the lab which discovered Adipose Derived Stem Cells (ADSC's). To my amazement, I received both positions and upon securing NIH project funding for the latter I headed to UCLA. Here, I met my mentor Dr. James Bradley and received support and experience from Drs. Bernard Sarnat and Henry Kawamoto. I will never forget the first question Dr. Bradley asked me; "Furlow developed his procedure

during residency, what are your ideas?" This provided my motivation for the rest of the year. My clinical projects included: Genioplasty Distraction with Hyoid Advancement among Treacher Collins and Nager Syndrome Patients for Resolution of Upper Airway Obstruction; Assessment of the Three Phases of Monobloc Advancement, Facial Artery Musculomucosal Flap for Closure of Large Nasal Septal Perforations, Posterior Fossa Box Reconstruction for Correction of Cerebellar Ptosis, Four Flap Z-Frenuloplasty for Correction of Severe Ankyloglossia, K-Stitch for Glabellar Width Reduction, and many others. Each of these projects proposed an innovative new approach and then assessed the new approach scientifically against other, more common, surgical methods. I truly believe that the beauty of Plastic Surgery lies within its innovation.

Along with these clinical projects, I was working in the ReBaR lab testing the effects of stress on osteogenic (bone) gene expression. Because we were unhappy with currently available systems of strain application, the engineering department helped us develop a new in-vitro distraction device (patent pending) that would apply a linear strain rather than a multi-dimensional strain (Chapter 3). Through the new applicator's use, I was able to demonstrate that strain significantly increased expression of osteogenic markers and decreased expression of bone formation inhibitors (e.g. Noggin) within the dura, periosteum, and osteogenic fronts of a suture (Chapter 1). Furthermore, when a normally patent suture was oscillated in this system, fusion could be induced. Utilizing the craniosynostotic rabbits from University of Pittsburgh, the same expression pattern was noted in craniosynostosis (Chapter 2). Clinically these findings explain why both a hydrocephalic child, when shunted, and a non-syndromic child, who experiences intra-uterine cephalic constriction, may present with craniosynostosis. At the time of this

discovery, I, along with Joubin Gabbay in Bioengineering, had also been working on a project in the ReBaR laboratories to optimize a scaffold so that we could achieve healing of critically sized femoral defects. Modifications had been made to the scaffold composition, structure, linked growth factors, and presence of ADSC's. The use of ADSC's had approached statistical significance for promotion of healing. To try and further improve this system, we used data from another experiment wherein preosteoblasts seeded in a collagen gel were stressed by our microdistractor and osteogenic gene expression was induced (Chapter 4). We then applied this system to ADSC's placed in a collagen gel and stressed via oscillation or distraction. In both instances a significant increase in osteogenic expression by the ADSC's was noted with strain. These strained cells are now being used in our femoral defects with very statistically significant results.

Outside the hospital and the lab, I have devoted many hours of my time coordinating various medicine related charities. The charities often focused on providing basic necessities and medical care to individuals who otherwise could not afford them. For example, I recently helped organize a benefit gala for UCLA's Facing Forward Foundation. The organization's main objective is to raise funds in order to provide craniofacial reconstruction to children whose families would not be able to afford the procedure. I helped manage the other volunteers to ensure that every facet of the evening was taken care of. This included everything from arranging the dinner menu to seeking donations for the auction. Through our efforts and hard work, the Facing Forward Foundation was able to raise nearly $100,000 by the end of the evening.

At the heart of all my actions, whether research, clinical or volunteer, my sole motivation lies in providing better care for patients. At Yale University and UCLA, I have experienced excellent training and mentorship, both of which have continually allowed me to grow as a doctor. I look forward to the tremendous opportunity to further pursue my ambitions of becoming a Plastic Surgeon.

Image taken in Chang Mai, Thailand during Yale Plastics Surgery Operation for Healing the Children.

REFERENCES

1. Cohen M. Craniosynostosis: diagnosis, evaluation, and management. New York: Raven Press, 1986.
2. Virchow R. Uber den Cretinismus, namentlich in Franken, und über pathologische Schädelformen. *Verh Phys Med Gesellsch Wurzburg*. 2: 230–270, 1851.
3. Graham JJ, Badura R, and Smith D. Coronal craniostenosis: fetal head constraint as one possible cause. *Pediatrics*. 65: 995–999, 1980.
4. Higginbottom M, Jones K, James H. Intrauterine constraint and craniosynostosis. *Neurosurgery*. 6: 39–44, 1980.
5. Wilkie A. Craniosynostosis: genes and mechanisms. *Hum Mol Genet*. 6: 1647–1656, 1997.
6. Cohen MJ. Sutural pathology. In: Cohen MJ and MacLean R, eds. Craniosynostosis: diagnosis, evaluation, and management. New York: Oxford University Press, 2000, p. 51–68.
7. DeLeon V, Jabs E, and Richtsmeier J. Craniofacial growth: genetic basis and morphogenetic process in craniosynostosis. In: Vander-Kolk C, ed. Craniomaxillofacial, cleft, and pediatric surgery. Philadelphia: Mosby. 2000, p. 619–636.
8. Wilkie A and Morriss-Kay G. Genetics of craniofacial development and malformation. *Nat Genet*. 2: 458–468, 2001.

9. Bellus GA, Gaudenz K, Zackai EH, et al. Identical mutations in three different fibroblast growth factor receptor genes in autosomal dominant craniosynostosis syndromes. *Nat Genet*. 14: 174–176, 1996.

10. Moloney DM, Wall SA, Ashworth GJ, et al. Prevalence of Pro250Arg mutation of fibroblast growth factor receptor 3 in coronal craniosynostosis. *Lancet*. 349: 1059- 1062, 1997.

11. Muenke M, Gripp K, McDonald-McGinn D, et al. A unique point mutation in the fibroblast growth factor receptor 3 gene (FGFR3) defines a new craniosynostosis syndrome. Am J Hum Genet. 60: 555–564, 1997.

12. Lajeunie E, El Ghouzzi V, Le Merrer M, et al. Sex related expressivity of the phenotype in coronal craniosynostosis caused by the recurrent P250R FGFR3 mutation. *J Med Genet*. 36: 9–13, 1999.

13. Graham J, DeSaxe M, and Smith D. Sagittal craniostenosis: fetal head constraint as one possible cause. *J Pediatr*. 95: 747–750, 1979.

14. Ferri J, Doual J, Kulik J, et al. Craniofacial behavior of sutures in young rabbits postimmobilization. *J Craniofac Surg*. 8: 483–489, 1997.

15. Bradley J, Shahinian H, Levine J, et al. Growth restriction of cranial sutures in the fetal lamb causes deformational changes, not craniosynostosis. *Plast Reconstr Surg*. 105: 2416–2423, 2000.

16. Opperman L, Sweeney T, Redmon J, et al. Tissue interactions with underlying dura mater inhibit osseous obliteration of developing cranial sutures. *Dev Dynam*. 198: 312–322, 1993.

17. Opperman L, Passarelli R, Morgan E, et al. Cranial sutures require tissue interactions with dura mater to resist osseous obliteration in vitro. *J Bone Miner Res*. 10: 1978–1987, 1995.

18. Opperman L, Chhabra A, Nolen A, et al. Dura mater maintains rat cranial sutures in vitro by regulating suture cell proliferation and collagen production. *J Craniofac Genet Dev Biol*. 18:150–158, 1998.

19. Pensler J, Ivescu A, and Radosevich J. Scaphocephaly: premature closure of the sagittal suture: a localized disorder of cellular metabolism? *Ann Plast Surg*. 40: 48–52, 1998.

20. Mooney M, Burrows A, Smith T, et al. Correction of coronal suture synostosis using suture and dura mater allografts in rabbits with familial craniosynostosis. *Cleft Palate Craniofac J*. 38: 206–225, 2001.

21. van der Klaauw C. Size and position of the functional components of the skull. *Arch Neerl Zool*. 9: 1–559, 1948–1952.

22. Moss M, Young R. A functional approach to craniology. *Am J Phys Anthropol*. 18: 281–202, 1960.

23. Moss M. The functional matrix. In: Kraus B and Reidel R, eds. Vistas in orthodontics. Philadelphia: Lea and Febiger. 1962, p 85–98.

24. Popa G. Mechanostruktur und mechanofunction der dura mater des menschen. *Morph J*. 78: 85–187, 1936.

25. Greenwald J, Mehrara B, Spector J, et al. Regional differentiation of cranial suture-associated dura mater in vivo and in vitro: implications for suture fusion and patency. *J Bone Miner Res*. 15: 2413–2430, 2000.

26. Hunenko O, Karmacharya J, Ong G, et al. Toward an understanding of nonsyndromic craniosynostosis: altered patterns of TGF-beta receptor and FGF receptor expression induced by intrauterine head constraint. *Ann Plast Surg*. 46: 546–553, 2001.

27. Kirschner R, Gannon F, Xu J, et al. Craniosynostosis and altered patterns of fetal TGF-beta expression induced by intrauterine constraint. *Plast Reconstr Surg*. 109: 2338–2346, 2002.

28. Mao JJ. Mechanobiology of craniofacial sutures. *J Dent Res*. 81: 810–816, 2002.

29. Mao JJ, Wang X, and Kopher RA. Biomechanics of craniofacial sutures: orthopedic implications. *Angle Orthod*. 73:128–135, 2003.

30. Mao JJ, Wang X, Mooney MP, et al. Strain induced osteogenesis of the craniofacial suture upon controlled delivery of low-frequency cyclic forces. *Front Biosci*. 8: A10–A17, 2003.

31. Ogle R, Tholpady S, McGlynn K, et al. Regulation of cranial suture morphogenesis. *Cells Tissues Organs*. 176: 54–66, 2004.

32. Schendel S, Walker G, and Kamisugi A. Hawaiian craniofacial morphometrics: average Mokapuan skull, artificial cranial deformation, and the "rocker" mandible. *Am J Phys Anthropol*. 52: 491–500, 1980.

33. Cheverud J, Kohn L, Konigsberg L, et al. Effects of frontooccipital artifical cranial vault modification on the cranial base and face. *Am J Phys Anthropol*. 88: 323–345, 1992.

34. Argenta LC, David LR, Wilson JA, et al. An increase in infant cranial deformity with supine sleeping position. *J Craniofac Surg*. 7:5–11, 1996.

35. Najarian SP. Infant cranial molding deformation and sleep position: implications for primary care. *J Pediatr Health Care*. 13: 173–177, 1999.

36. Babler WJ, Persing JA: Changes in facial and basicranial dimensions related to premature closure of the coronal suture in rabbits. *Anat Rec* 199: 14A, 1981.

37. Moss M. The pathogenesis of premature cranial synostosis in man. *Acta Anat*. 37: 351–370, 1959.

38. Blechschmidt, M. Biokinetics of the developing basicranium. In: Bosma J, ed. Symposium on development of the basicranium. Bethesda: U.S. Department of Health, Education, and Welfare, 1976, p 44–53.

39. Siebert J, Kokich V, Warkany J, et al. Atelencephalic microcephaly: craniofacial anatomy and morphologic comparisons with holoprosencephaly and anencephaly. *Teratology*. 36: 279–285, 1987.

40. Kjaer I. Human prenatal craniofacial development related to brain development under normal and pathologic conditions. *Acta Odontol Scand*. 53: 135–143, 1995.

41. Trenouth M. Alteration in facial shape in the anencephalic human fetus. *Br J Orthod*. 23: 129–136, 1996.

42. Garg B and Walsh L. Clinical approach to the child with a large head. *Ind J Pediatr*. 68: 867–871, 2001.

43. Marchac, D., and Renier, D. Craniosynostosis. *World J. Surg.* 13: 358, 1989.

44. McCarthy, J. G., Epstein, F. J., and Wood-Smith, D. Craniosynostosis. In J. G. McCarthy (Ed.), *Plast. Surg*. Philadelphia: Saunders, 1990. Pp. 3013-3053.

45. Robin, N. H. Molecular genetic advances in understanding craniosynostosis. *Plast. Reconstr. Surg.* 103: 1060, 1999.

46. Levine J.P., Bradley J.P., Roth D.A., et al. Studies in cranial suture biology: regional dura mater determines overlying suture biology. *Plast. Reconstr. Surg.* 101:1441, 1998.

47. Roth, D.A., Bradley, J.P., Levine, J.P., et al. Studies in cranial suture biology: II. Role of dura in cranial suture fusion. *Plast. Reconstr. Surg.* 97: 693, 1996.

48. Law, C.S., Warren, S.M., Mehrara, B.J., et al. Gene expression profiling in the rat cranial suture. *J Craniofac. Surg.* 16: 378, 2005.

49. Opperman, L.A., Nolen, A.A., and Ogle, R.C. TGF-beta 1, TGF-beta 2, and TGF-beta 3 exhibit distinct patterns of expression during cranial suture formation and obliteration in vivo and in vitro. *J Bone Miner Res.* 12: 301, 1997.

50. Roth, D.A., Longaker, M.T., and McCarthy, J.G. Studies in cranial suture biology: Part I. Increased immunoreactivity for trans-forming growth factor-beta (1, b 2, b 3) during rat cranial suture fusion. *J Bone Miner Res.* 12: 311, 1997.

51. Roth, D.A., Gold, L.I., Han, V.K., et al. Immunolocalization of trans-forming growth factor beta 1, beta 2, and beta 3 and insulin-like growth factor I in premature cranial suture fusion. *Plast Reconstr. Surg.* 99: 300, 1997.

52. Mehrara, B.J., Most, D.E., Chang, J., et al. Basic fibroblast growth factor and transforming growth factor beta-1 expression in the developing dura mater correlates with calvarial bone formation. *Plast. Reconstr. Surg.* 102: 1805, 1999.

53. Mehrara, B.J., Steinbrech, D.S., Saadeh, P.B., et al. Expression of high-affinity receptors for TGF-beta during rat cranial suture fusion. *Ann Plast Surg.* 42: 502, 1999.

54. Kim, H., Rice, D.P., Kettunen, P.J., et al. FGF-, BMP- and Shh-mediated signaling pathways in the regulation of cranial suture morphogenesis and calvarial bone development. *Development*. 125: 1241, 1998.

55. Opperman, L.A., Adab, K., and Gakunga, P.T. Tgf- b2 and Tgf- b3 regulate fetal rat cranial suture morphogenesis by regulating rates of cell proliferation and apoptosis. *Dev Dyn.* 219: 237, 2000.

56. Opperman, L.A., Chhabra, A., Cho, R.W., et al. Cranial suture obliteration is induced by removal of transforming growth factor (Tgf)-beta 3 activity and prevented by removal of Tgf-beta 2 activity from fetal rat calvaria in vitro. *J Craniofac Genet Dev Biol.* 19: 164, 1999.

57. Opperman, L.A., Moursi, A.M., Sayne, J.R., et al. Tgf-b3 in collagen gel delays fusion of rat posterior frontal suture in vivo. *Anat Rec.* 267: 120, 2002.

58. Opperman, L.A., Nolen, A.A., and Ogle, R.C. Tgf-b1, Tgf-b2, and Tgf-b3 exhibit distinct patterns of expression during cranial suture formation and obliteration *in vivo* and *in vitro. J Bone Miner Res.* 12: 301, 1997.

59. Warren, S.M., Brunet, L.J., Harland, R.M., et al. The BMP antagonist noggin regulates cranial suture fusion. *Nature*. 422: 625, 2003.

60. Park, M.H., Shin, H.I., Choi, J.Y., et al. Differential expression patterns of Runx2 \isoforms in cranial suture morphogenesis. *J Bone Miner Res.* 16: 885, 2001.

61. Ogle, R.C., Tholpady, S.S., McGlynn, K.A., et al. Regulation of cranial suture morphogenesis. *Cells Tissues organs.* 176: 54, 2004.

62. Yu, J.C., Lucas, J.H., Fryberg, K., et al. Extrinsic Tension Results in FGF-2 Release, membrane permeability change, and intracellular Ca++ increase in immature cranial sutures. *J Craniofac Surg.* 12: 391, 2001.

63. Kirschner, R.E., Gannon, F.H., Xu, J., et al. Craniosynostosis and altered patterns of fetal TGF-beta expression induced by intrauterine constraint. *Plast. Reconstr. Surg.* 109: 2338, 2002.

64. Moss, M. Inhibition and Stimulation of of sutural fusion in the rat calvaria. *Anat. Rec.* 136: 457, 1960.

65. Bradley, J.P., Levine, J.P., McCarthy, J.G., et al. Studies in cranial suture biology: Regional dura mater determines *in-vitro* cranial suture fusion. *Plast. Reconstr. Surg.* 100: 1091, 1997.

66. Kim, H.J., Kettunen, P.J., and Thesleff, I. FGF-, BMP-, and Shh- mediated pathways in the regulation of cranial suture morphogenesis and calvarial bone development. *Development.* 125: 1241, 1998.

67. Law, C.S., Warren, S.M., Mehrara, B.J., et al. Gene expression profiling in the rat cranial suture. *J of Craniofac Surg.* 16: 378, 2005.

68. Ikegame, M., Ishibashi, O., Yoshizawa, T., et al. Tensile stress induces bone morphogenetic protein 4 in preosteoblastic and fibroblastic cells, which later differentiate into osteoblasts leading to Osteogenesis in the mous calvaria in organ culture. *J Bone & Miner Res.* 16: 24, 2001.

69. Chen, D., Zhao, M., and Mundy, G. Bone morphogenetic proteins. *Growth Factors*. 22: 233, 2004.

70. Cohen MM Jr.: Craniosynostosis update 1987. *Am J Med Genet Suppl* 1988;4:99-148.

71. Holleville N, Ouilhac A, Bontoux M, et al. BMP signals regulate D1x5 during early avian skull development. *Dev Biol.* 2003;257:177-189.

72. Warren SM., Brunet LJ, Harland RM, et al. The BMP antagonist noggin regulates cranial suture fusion. *Nature*. 2003;422:625-629.

73. Groppe J, Greenwald J, Wiater E, et al. Structural basis of BMP signaling inhibition by Noggin, a novel twelve-membered cystine knot protein. *J Bone Joint Surg Am.* 2003;85-A suppl 3:52-58.

74. Park MH, Shin HI, Choi JY, et al. Differential expression patterns of Runx2 isoforms in cranial suture morphogenesis. *J Bone Miner Res*. 2001;16:885-92.

75. Mooney MP, Losken HW, Siegel MI, et al. Development of a strain of rabbits with congenital simple nonsyndromic coronal suture synostosis. Part II: Somatic and craniofacial growth patterns. *Cleft Pal. Craniofac. J*. 1994;31:8-16.

76. Mooney MP, Siegel MI, Burrows AM, et al. A rabbit model of human familial, nonsyndromic unicoronal suture synostosis. II. Intracranial contents, intracranial volume, and intracranial pressure. *Child's Nerv. Sys*. 1998;14:247-255.

77. Opperman LA, Passarelli RW, Morgan EP, et al. Cranial sutures require tissue interactions with dura mater to resist osseous obliteration in vitro. *J. Bone Miner. Res.* 1995;10:1978-87.

78. Bradley JP, Levine JP, McCarthy JG, et al. Studies in Cranial Suture Biology: Regional Dura Mater Determines in Vitro Cranial Suture Fusion. *Plast Reconstr Surg*. 1997;100:1091-1099.

79. Roth DA, Bradley JP, Levine JP, et al. Studies in cranial suture biology: part II. Role of the dura in cranial suture fusion. *Plast. Reconstr. Surg.* 1996;97:693-9.

80. Zimmerman LB, De Jesus-Escobar JM, Harland RM. The Speeman organizer signal noggin binds and inactivates bone morphogenetic protein 4. *Cell* 1996;86:599-606.

81. Urist MR. Bone morphogenetic protein: the molecularization of skeletal system development. *J Bone Miner Res*. 1997;12:343-346.

82. Chen D, Zhao M, Mundy G. Bone morphogenetic proteins. *Growth Factors* 2004;22:233-41.

83. Nacamuli RP, Fong KD, Warren SM, et al. Markers of Osteoblast Differentiation in Fusing and Nonfusing Cranial Sutures. *Plast. Reconstr. Surg*. 2003;112:1328-1335.

84. McCarthy, JG (ed.). Distraction of the craniofacial skeleton. Springer. New York. 1999

85. Ilizarov, GA. Clinical application of the tension-stress effect for limb-lenghtening. *Clin Orthop.* 250: 8-26, 1990.

86. Vadiakas GP, Banes AJ. Verapamil decreases cyclic load-induced calcium incorporation in ROS 17/2.8 osteosarcoma cell cultures. *Matrix.* 12: 439, 1992.

87. Harter LV, Hruska KA, and Duncan RL. Human Osteoblast-Like Cells Respond to Mechanical Strain with Increased Bone Matrix Protein Production Independent of Hormonal Regulation. *Endocrinology* 136: 528-535, 1995.

88. Cillo JE, Gassner R, Koepsel RR, and Buckley MJ. Growth factor and cytokine gene expression in mechanically strained human osteoblast-like cells: implications for distraction osteogenesis. *Oral Surg Oral Med Oral Pathol Oral Radiol Endod*. 90: 147, 2000.

89. Gosain AK, Song LS, Santoro T, Weihrauch D, Bosi BO, Corrao MA, Chilian WM. Effects of transforming growth factor factor-[beta] and mechanical strain on osteoblast cell counts: an *in vitro* model for distraction osteogenesis. *Plast Reconstr Surg*. 105(1):130-136. 2000.

90. Buckley MJ, Banes AJ, and Jordan RD. The effects of mechanical strain on osteoblasts *in vitro. J Oral Maxillofac Surg.* 48: 276, 1990.

91. Carvalho RS, Scott JE, Saga DM, Yen EH. Stimulation of signal tranduction pathways in osteoblasts by mechanical strain potentiated by parathyroid hormone. *Journal of Bone & Mineral Research.* 9: 999, 1994.

92. Carvalho RS, Scott JE, Yen EH. The effect of mechanical stimulation on distribution of beta-1 integrin and expression of beta 1-integrin mRNA in TE-85 human osteosarcoma cells. *Archives of Oral Biology.* 40: 257. 1995.

93. Carvalho RS, Bumann A, Schwarzer C, Scott JE, Yen EH. A molecular mechanism of integrin regulation from bone cells stimulated by orthodontic forces. European Journal of Orthodontics. 18: 227, 1996.

94. Banes AJ, Gilbert J, Taylor D, and Monbureau O. A new vacuum-operated stress-providing instrument that applies static or variable duration cyclic tension or compression to cells *in vitro*. J Cell Sci. 75: 35, 1985.

95. Knezevic V, Sim AJ, Borg TK, and Holmes JW. Isotonic biaxial loading of fibroblast-populated collagen gels: a versatile, low-cost system for the study of mechanobiology. *Biomechan Model Mechanobiol*. 1: 59, 2002.

96. Beck G, Sullivan E, Moran, Zerler. Relationship between alkaline phosphatase levels, osteopontin expression and mineralization in differentiating MC3T3-E1 Osteoblasts. Journal of Cellular Biochemistry 68: 260-280 (1998).

97. Ilizarov GA, Ledioev VI, and Shitin VP. The course of compact bone reparative regeneration in distraction osteosynthesis under different conditions of bone fragment fixation and experimental study. *Exp. Khir. Anest*. 14:3, 1969.

98. Yu J, Fearon J, Havlik R, Buchman S, Polley J. Distraction Osteogenesis of the Craniofacial Skeleton. 114: 1e, 2004.

99. Paccione M, Mehrara B, Warren S, Greenwald J, Spector J, Luchs J, Longaker M. Rat Mandibular Distraction Osteogenesis: Latency, Rate, Rhythm Determine the Adaptive Response. Journal of Craniofacial Surgery. 12 (2): 175-182, March 2001.

100. Matsuno M, Hata K, Sumi Y, Mizuno H, Ueda M. *In vitro* analysis of distraction osteogenesis. Journal of Craniofacial Surgery. 2000 July; 11(4) 303-307.

101. Choi IH, Ahn JH, Chung CY, Cho TJ. Vascular proliferation and blood supply during distraction osteogenesis: a scanning electron microscopic observation. Journal Orthopedic Research 2000 Sep; 18 (5): 698-705.

102. Greenwald J, Luchs J, Mehrara B, Spector J, Mackool R.J., McCarthy J, Longaker M. "Pumping the Regenerate". An evaluation of Oscillating Distraction Osteogenesis in the Rodent Mandible. *Annals of Plast Surg* 2000; 44:516-521.

103. Martin RB (2000) Toward a unifying theory of bone remodeling. Bone 26:1–6.

104. Duncan RL, Turner CH (1995) Mechanotransduction and the functional response of bone to mechanical strain. Calcif Tissue Int 57:344–358.

105. Turner CH, Pavalko FM (1998) Mechanotransduction and functional response of the skeleton to physical stress: the mechanisms and mechanics of bone adaptation. J Orthop Sci 3:346–355.

106. Rawlinson SC, Pitsillides AA, Lanyon LE (1996) Involvement of different ion channels in osteoblasts' and osteocytes' early responses to mechanical strain. Bone 19:609–614.

107. Kawata A, Mikuni-Takagaki Y (1998) Mechanotransduction in stretched osteocytes—temporal expression of immediate early and other genes. Biochem Biophys Res Commun 246:404–408.

108. Stanford CM, Welsch F, Kastner N, Thomas G, Zaharias K, Holtman K, Brand RA (2000) Primary human bone cultures from older patients do not respond at continuum levels of in vivo strain magnitudes. J Biochem 33:63–71.

109. Owan I, Burr DB, Turner CH, Qiu J, Tu Y, Onyia JE, Duncan RL (1997) Mechanotransduction in bone: osteoblasts are more responsive to fluid forces than mechanical strain. Am J Physiol 273:C810–815.

110. Jacobs CR, Yellowley CE, Davis BR, Zhou Z, Cimbala HJ, Donahue HJ (1998) Differential effect of steady versus oscillating flow on bone cells. J Biomech 31:969–976.

111. Kaspar D, Seidl W, Neidlinger-Wilke C, Ignatius A, Claes L. Dynamic cell stretching increases human osteoblast proliferation and CICP synthesis but decreases osteocalcin synthesis and alkaline phosphatase activity. J Biomech. 2000;33:45-51.

112. Frost HM. From Wolff's law to the Utah paradigm: insights about bone physiology and its clinical applications. Anat Rec. 2001;262:398-419.

113. Skerry TM, Suva LJ. Investigation of the regulation of bone mass by mechanical loading: from quantitative cytochemistry to gene array. Cell Biochem Funct. 2003;21:223-9

114. Pearson OM, Lieberman DE. The aging of Wolff's "law": Ontogeny and responses to mechanical loading in cortical bone. Am J Phys Anthropol. 2004;Suppl 39:63-99.

115. Buckley MJ, Banes AJ, and Jordan RD. The effects of mechanical strain on osteoblasts *in vitro.* J Oral Maxillofac Surg. 48: 276, 1990.

116. Carvalho RS, Scott JE, Yen EH. The effect of mechanical stimulation on distribution of beta-1 integrin and expression of beta 1-integrin mRNA in TE-85 human osteosarcoma cells. *Archives of Oral Biology.* 40: 257. 1995.

117. Harter LV, Hruska KA, and Duncan RL. Human Osteoblast-Like Cells Respond to Mechanical Strain with Increased Bone Matrix Protein Production Independent of Hormonal Regulation. *Endocrinology* 136: 528-535, 1995.

118. Carvalho RS, Bumann A, Schwarzer C, Scott JE, Yen EH. A molecular mechanism of integrin regulation from bone cells stimulated by orthodontic forces. European Journal of Orthodontics. 18: 227, 1996.

119. Kinoshita S, Finnegan M, Bucholz RW, Mizuno K. Three-dimensional collagen gel culture promotes osteoblastic phenotype in bone marrow derived cells. Kobe J Med Sci. 1999;45:201-11.

120. Cillo JE, Gassner R, Koepsel RR, and Buckley MJ. Growth factor and cytokine gene expression in mechanically strained human osteoblast-like cells: implications for distraction osteogenesis. Oral Surg Oral Med Oral Pathol Oral Radiol Endod. 90: 147, 2000.

121. Gosain AK, Song LS, Santoro T, Weihrauch D, Bosi BO, Corrao MA, Chilian WM. Effects of transforming growth factor factor-[beta] and mechanical strain on osteoblast cell counts: an *in vitro* model for distraction osteogenesis. Plast Reconstr Surg. 105(1):130-136. 2000.

122. Gerber I, ap Gwynn I. Differentiation of rat osteoblast-like cells in monolayer and micromass cultures. Eur Cell Mater. 2002;3:19-30.

123. Weismann PS, Nazer N, Klatt C, Szuwart T, Meyer U. Bone tissue engineering by primary osteoblast-like cells in a monolayer system and 3-dimensional collagen gel. J Oral Maxillofac Surg. 2003;61:1455-62.

124. Askari M, Gabbay JS, Tahernia A, O'Hara CM, Heller JB, Azari K, Hollinger JO, Bradley JP. Favorable morphologic change of preosteoblasts in a 3-dimensional matrix with *in vitro* microdistraction. Plas Reconstr Surg. In Press.

125. Liu F, Malaval L, Gupta AK, Aubin JE. Simultaneous detection of multiple bone-related mRNAs and protein expression during osteoblast differentiation: polymerase chain reaction and immunocytochemical studies at the single cell level. Dev Biol. 1994;166:220-34.

126. Beck GR Jr, Sullivan EC, Moran E, Zerler B. Relationship between alkaline phosphatase levels, osteopontin expression, and mineralization in differentiating MC3T3-E1 osteoblasts. J Cell Biochem. 1998;68:269-80.

127. Sato M, Yasui N, Nakase T, Kawahata H, Sugimoto M, Hirota S, Kitamura Y, Nomura S, Ochi T. Expression of bone matrix proteins mRNA during distraction osteogenesis. J Bone Miner Res. 1998;13:1221-31.

128. Mehrara BJ, Rowe NM, Steinbrech DS, Dudziak ME, Saadeh PB, McCarthy JG, Gittes GK, Longaker MT. Rat mandibular distraction osteogenesis: II. Molecular analysis of transforming growth factor beta-1 and osteocalcin gene expression. Plast Reconstr Surg. 1999;103:536-47.

129. Nomura S, Takano-Yamamoto T. Molecular events caused by mechanical stress in bone. Matrix Biol. 2000;19:91-6.

130. Bouletreau PJ, Warren SM, Longaker MT. The molecular biology of distraction osteogenesis. J Craniomaxillofac Surg. 2002;30:1-11.

131. Carvalho RS, Schaffer JL, Gerstenfeld LC. Osteoblasts induce osteopontin expression in response to attachment on fibronectin: demonstration of a common role for integrin receptors in the signal transduction processes of cell attachment and mechanical stimulation. J Cell Biochem. 1998;70:376-90.

132. Kaspar D, Seidl W, Neidlinger-Wilke C, Ignatius A, Claes L. Dynamic cell stretching increases human osteoblast proliferation and CICP synthesis but decreases osteocalcin synthesis and alkaline phosphatase activity. J Biomech. 2000;33:45-51.

133. Walker LM, Publicover SJ, Preston MR, Said Ahmed MA, El Haj AJ. Calcium-channel activation and matrix protein upregulation in bone cells in response to mechanical strain. J Cell Biochem. 2000;79:648-61.

134. Lee DH, Park JC, Suh H. Effect of centrifugal force on cellular activity of osteoblastic MC3T3-E1 cells in vitro. Yonsei Med J. 2001;42:405-10.

135. Carvalho RS, Bumann A, Schaffer JL, Gerstenfeld LC. Predominant integrin ligands expressed by osteoblasts show preferential regulation in response to both cell adhesion and mechanical perturbation. J Cell Biochem. 2002;84:497-508.

136. Fong KD, Nacamuli RP, Loboa EG, Henderson JH, Fang TD, Song HM, Cowan CM, Warren SM, Carter DR, Longaker MT. Equibiaxial tensile strain affects calvarial osteoblast biology. J Craniofac Surg. 2003 May;14(3):348-55.

137. Pioletti DP, Muller J, Rakotomanana LR, Corbeil J, Wild E. Effect of micromechanical stimulations on osteoblasts: development of a device simulating the mechanical situation at the bone-implant interface. J Biomech. 2003;36:131-5.

138. Ignatius A, Blessing H, Liedert A, Schmidt C, Neidlinger-Wilke C, Kaspar D, Friemert B, Claes L. Tissue engineering of bone: effects of mechanical strain on osteoblastic cells in type I collagen matrices. Biomaterials. 2005;26:311-8.

139. Akhouayri O, Lafage-Proust MH, Rattner A, Laroche N, Caillot-Augusseau A, Alexandre C, Vico L. Effects of static or dynamic mechanical stresses on

osteoblast phenotype expression in three-dimensional contractile collagen gels. J Cell Biochem. 1999;76:217-30.

140. Nagatomi J, Arulanandam BP, Metzger DW, Meunier A, Bizios R. Frequency- and duration-dependent effects of cyclic pressure on select bone cell functions. Tissue Eng. 2001;7:717-28.

141. Jiang GL, White CR, Stevens HY, Frangos JA. Temporal gradients in shear stimulate osteoblastic proliferation via ERK1/2 and retinoblastoma protein. Am J Physiol Endocrinol Metab. 2002;283:E383-9.

142. Kaspar D, Seidl W, Neidlinger-Wilke C, Beck A, Claes L, Ignatius A. Proliferation of human-derived osteoblast-like cells depends on the cycle number and frequency of uniaxial strain. J Biomech. 2002;35:873-80.

143. Di Palma F, Douet M, Boachon C, Guignandon A, Peyroche S, Forest B, Alexandre C, Chamson A, Rattner A. Physiological strains induce differentiation in human osteoblasts cultured on orthopaedic biomaterial. Biomaterials. 2003;24:3139-51.

144. Kapur S, Baylink DJ, Lau KH. Fluid flow shear stress stimulates human osteoblast proliferation and differentiation through multiple interacting and competing signal transduction pathways. Bone. 2003;32:241-51.

145. Walboomers XF, Habraken WJ, Feddes B, Winter LC, Bumgardner JD, Jansen JA. Stretch-mediated responses of osteoblast-like cells cultured on titanium-coated substrates in vitro. J Biomed Mater Res A. 2004;69:131-9.

146. Jessop HL, Rawlinson SC, Pitsillides AA, Lanyon LE. Mechanical strain and fluid movement both activate extracellular regulated kinase (ERK) in osteoblast-like cells but via different signaling pathways. Bone. 2002;31:186-94.

147. Kubota T, Yamauchi M, Onozaki J, Sato S, Suzuki Y, Sodek J. Influence of an intermittent compressive force on matrix protein expression by ROS 17/2.8 cells, with selective stimulation of osteopontin. Arch Oral Biol. 1993 Jan;38(1):23-30.

148. Toma CD, Ashkar S, Gray ML, Schaffer JL, Gerstenfeld LC. Signal transduction of mechanical stimuli is dependent on microfilament integrity: identification of osteopontin as a mechanically induced gene in osteoblasts. J Bone Miner Res. 1997;12:1626-36.

149. Perrien DS, Brown EC, Aronson J, Skinner RA, Montague DC, Badger TM, Lumpkin CK Jr. Immunohistochemical study of osteopontin expression during distraction osteogenesis in the rat. J Histochem Cytochem. 2002;50:567-74.

150. Fang TD, Nacamuli RP, Song HM, Fong KD, Warren SM, Salim A, Carano RA, Filvaroff EH, Longaker MT. Creation and characterization of a mouse model of mandibular distraction osteogenesis. Bone. 2004;34:1004-12.

151. Tong L, Buchman SR, Ignelzi MA Jr, Rhee S, Goldstein SA. Focal adhesion kinase expression during mandibular distraction osteogenesis: evidence for mechanotransduction. Plast Reconstr Surg. 2003;111:211-22

152. Graham JM, deSaxe M, Smith DW: Sagittal craniostenosis: Fetal head constraint as one possible cause. J Pediatr 95: 747-750, 1979.